Estimation of boreal forest canopy cover with ground measurements, statistical models and remote sensing

Lauri Korhonen
School of Forest Sciences
Faculty of Science and Forestry
University of Eastern Finland

Academic dissertation

To be presented, with the permission of the Faculty of Science and Forestry of the University of Eastern Finland, for public criticism in the auditorium BOR100 of the University of Eastern Finland, Yliopistokatu 7, Joensuu, on 15th April 2011, at 12 o'clock noon.

Title of dissertation: Estimation of boreal forest canopy cover with ground measurements, statistical models and remote sensing

Author: Lauri Korhonen

Thesis supervisors:
Dr. Kari T. Korhonen
Finnish Forest Research Institute, Joensuu Research Unit, Joensuu, Finland
Prof. Matti Maltamo
School of Forest Sciences, University of Eastern Finland, Joensuu, Finland
Prof. Pauline Stenberg
Department of Forest Sciences, University of Helsinki, Helsinki, Finland

Pre-examiners:
Dr. Inge Jonckheere
FAO HQ - Climate Change, Rome, Italy
Dr. Klemens Schadauer
Institut für Waldinventur, Vienna, Austria

Opponent:
Dr. Jari Varjo
Finnish Forest Research Institute, Vantaa Research Unit, Vantaa, Finland

ABSTRACT

Forest canopy cover (CC) is an important ecological variable and the basis for the international definition of forest. Canopy cover is defined as the proportion of forest floor covered by the vertical projection of the tree crowns. Thus, an unbiased estimation of CC requires that the area of interest is covered by vertical measurements, typically by using upward-looking sighting tubes. However, these measurements are very laborious. In practical forest inventories the estimate should be obtained as quickly as possible, but large errors should still be avoided. The aim of this thesis was to compare different quicker-to-apply CC estimation techniques to more accurate sighting tube estimates. One alternative is to use instruments with an angle of view (AOV), such as cameras or spherical densiometers, instead of the sighting tubes. This may, however, lead to biased results when using large AOVs, because the sides of the crowns are also observed. The results showed that moderate (max. 40°) AOVs can be used to decrease the number of required sample points without causing a large bias, but more than 20 measurements per plot should be made to avoid large errors in all forests. A new instrument, the crown relascope, is potentially a good alternative in low cover forests where the trees are not very tall. Ocular estimates were found to depend on the observer, but considerable underestimation of CC was common. Furthermore, models for predicting CC based on commonly available forest metrics such as tree height and basal area were created, and reached a precision similar to the quicker field methods. Finally, airborne laser scanning data can be used to estimate CC from the proportion of pulses that hit the canopy above a predefined height limit. The laser method was found to have a high precision but resulted in a small overestimation of CC.

Keywords: Canopy cover; canopy closure; Cajanus tube; beta regression; image processing; LiDAR

ACKNOWLEDGEMENTS

LIST OF ORIGINAL ARTICLES

This thesis is based on the following articles, referred to according to their Roman numerals:

I. Korhonen, L., Korhonen, K.T., Rautiainen, M & Stenberg, P. 2006. Estimation of forest canopy cover: a comparison of field measurement techniques. Silva Fennica 40(4): 577–588. http://www.metla.fi/silvafennica/full/sf40/sf404577.pdf

II. Korhonen, L., Korhonen, K.T., Stenberg, P., Maltamo, M. & Rautiainen, M. 2007. Local models for forest canopy cover with beta regression. Silva Fennica 41(4): 671–685. http://www.metla.fi/silvafennica/full/sf41/sf414671.pdf

III. Stenberg, P., Korhonen, L. & Rautiainen, M. 2008. A relascope for measuring canopy cover. Canadian Journal of Forest Research 38(9): 2545–2550. http://dx.doi.org/10.1139/X08-081

IV. Korhonen, L. & Heikkinen, J. 2009. Automated analysis of in situ canopy images for the estimation of forest canopy cover. Forest Science 55(4): 323–334. http://www.ingentaconnect.com/content/saf/fs/2009/00000055/00000004/art00004

V. Korhonen, L., Korpela, I., Heiskanen, J. & Maltamo, M. Airborne discrete-return LiDAR data in the estimation of vertical canopy cover, angular canopy closure and leaf area index. Remote Sensing of Environment 115(4): 1065-1080. http://dx.doi.org/10.1016/j.rse.2010.12.011

The articles are reprinted with kind permission of the publishers.

Studies I–II: Korhonen was responsible for the field data collection, its analysis and writing, while other authors participated in the planning and manuscript preparation.

Study III: Korhonen was responsible for the field data collection and analysis, and participated in the writing.

Study IV: Heikkinen wrote the original Matlab source code, while Korhonen collected the field data, analyzed it and wrote the study.

Study V: Korhonen collected and processed most of the field data, processed the LiDAR data with self-written software, and wrote most of the study.

6

CONTENTS

ABBREVIATIONS

AIC	Akaike information criterion
AOV	Angle of view
BAF	Basal area factor of a relascope
CBAF	Crown basal area factor
CC	Canopy cover
CI	Confidence interval
CHM	Canopy height model
FAO	Food and Agriculture Organization of the United Nations
FCI	First echo cover index, i.e. the laser-derived proportion of first echo canopy hits
GLM	Generalized linear model
GPS	Global positioning system
IPCC	Intergovernmental Panel on Climate Change
L_{max}, L_{min}	Upper and lower confidence limits
LiDAR	Light detection and ranging
NDVI	Normalized difference vegetation index
NFI	National forest inventory
Radar	Radio detection and ranging
REDD	Reducing emissions from deforestation and forest degradation in developing countries
RMSE	Root mean squared error
sd	Standard deviation
SPOT	Satellite pour l'observation de la terre
SRS	Simple random sampling
TLS	Terrestrial laser scanning

ERRATA

Study I

In the decimation of the Cajanus tube dot count data down to 49 and 23 points per plot, the results were incorrect for five plots (18, 22, 24, 40, and 56). Thus, the outliers at Caj. 49 and Caj. 23 columns in Figure 3 disappear. The correct rows two and three in Table 2 are:

Method	N	Mean	Median	Std. dev.	Quartile range	Min	Max
Cajanus tube 49 points	19	0.002	0.011	0.048	0.061	-0.085	0.084
Cajanus tube 23 points	19	-0.016	-0.023	0.074	0.105	-0.160	0.145

The corrections led to lower standard deviations and smaller underestimations in these cases. The correct results of the Kruskall-Wallis test still indicate that the H_0 of equal medians was rejected ($\chi^2 = 59.2$, d.f. = 13, P < 0.01). The correct table of multiple comparisons is given below. The conclusions did not change significantly.

Method	N	Mean rank	Difference from control	Standard error	Test coefficient
Cajanus 195 points (control)	19	149.0	0.0	12.15	0.00
Cajanus 102 points	19	160.3	11.3	12.15	0.93
Cajanus 49 points	19	154.8	5.8	12.15	0.48
Cajanus 23 points	19	133.7	-15.3	12.15	-1.26
LIS	19	144.8	-4.2	12.15	-0.34
Densiometer 49 points	19	162.9	13.9	12.15	1.14
Densiometer 23 points	19	156.0	7.0	12.15	0.58
Densiometer 9 points	19	137.3	-11.7	12.15	-0.96
Densiometer 10 points subjective sample	19	103.1	-45.9	12.15	-3.78[a]
Digital photographs	18	63.8	-85.2	12.31	-6.92[a]
Black-painted digital photographs	18	156.5	7.5	12.31	0.61
A's ocular estimate	14	154.4	5.4	13.04	0.41
B's ocular estimate	19	98.8	-50.2	12.15	-4.13[a]
C's ocular estimate	19	48.8	-100.2	12.15	-8.24[a]

[a]Statistically significant difference at α=0.05 (critical value 2.891).

The horizontal and vertical angles of view of the camera were 63° and 49°, respectively.

Johansson's paper should be cited with the year 1985, not 1984.

Reference: Zar, J. H. 1984. Biostatistical analysis. 2nd ed. Prentice-Hall, Inc., Englewood Cliffs, New Jersey, is missing from the list of references.

Study IV

Equation 5 should be written as follows:

$$RMSE = \sqrt{\frac{\sum_{i=1}^{n}(y_i - \hat{y}_i)^2}{n}}$$

1 INTRODUCTION

1.1 Background

The usual aim of forest inventories is to provide information on the timber volume and the need for management in the area of interest. In addition to the economic requirements, modern forest inventories must also produce data concerning ecological and social aspects of forestry. From the ecological perspective, the canopy can be considered to be the most important part of a forest ecosystem. For instance, Ozanne et al. (2003, p. 183) stated that "the forest canopy is the functional interface between 90% of Earth's terrestrial biomass and the atmosphere" and, in addition, that it "plays a crucial role in the maintenance of biodiversity". Because of this, the parameters that can be used to describe canopy structure and functioning need to be estimated. Canopy cover (CC) is one example of a commonly used indicator of canopy structure.

Canopy cover is traditionally defined as the proportion of ground covered by the vertical projection of the tree crowns (Jennings et al. 1999). Numerous studies stated the usefulness of canopy cover as an indicator of plant and animal habitats (e.g. Anderson et al. 1969, James 1971, Werner and Glennemeier 1999, Ranius and Jansson 2000). In forest management, CC can be used as a measure of stand density (Zeide 2005) and thus it can be utilized in silvicultural decision making (Johansson 1985, Buckley et al. 1999). Forest fire severity can be quantified as a change in CC (Miller et al. 2009). Ancillary canopy cover data is also useful in the development of different remote sensing methods, as it describes which proportion of the signal originates from the canopy (Jasinski 1990, Spanner et al. 1990, Rautiainen et al. 2003, Stenberg et al. 2008). Similarly, CC influences the Earth's surface albedo, and thus the climate both locally and globally (Betts and Ball 1997, Lohila et al. 2010).

Finally, the main reason for the inclusion of canopy cover in most national forest inventories (NFIs) is the fact that the international definition of forest is based on canopy cover. The FAO (2004, p. 17) defines forest as

"Land spanning more than 0.5 hectares with trees higher than 5 meters and a canopy cover of more than 10 percent, or trees able to reach these thresholds *in situ*. It does not include land that is predominantly under agricultural or urban land use."

Consequently, CC measurements and models are needed to calculate national forest areas for international forest statistics. Forest area monitoring has become especially important in developing countries after the initiation of the REDD (Reducing Emissions from Deforestation and Forest Degradation in Developing Countries) mechanism (GOFC-GOLD 2009). Deforestation and forest degradation cause greenhouse gas emissions, and therefore the REDD mechanism was introduced as a means to provide financial compensation for the countries that preserve their forests. Changes in CC may also indicate forest degradation, for example illegal loggings (GOFC-GOLD 2009). Intergovernmental Panel on Climate Change has defined three different tier levels that describe the precision of the forest information (IPCC 2006). High tier level means more reliable forest data and warrants higher compensation, if the forest area remains larger than a predefined baseline suggests. Thus the quality of CC data obtained from field measurements and remote sensing has become extremely important.

1.2 Concepts related to canopy cover measures

The terminology that has been used to describe different forest cover metrics and measurements in the literature has been very vague (Jennings et al. 1999, Wilson 2011). There are many concepts that appear to be synonymous to concept canopy cover: canopy closure, crown cover, crown closure, fractional cover, and canopy density, amongst others. In addition, antonyms such as canopy gap fraction and canopy openness are commonly used. The problem is that different mensuration techniques produce different cover estimates. For example, instruments that observe a large area of the canopy from each point, such as cameras equipped with fisheye lenses, produce larger cover estimates than sighting tubes that measure the canopy in a vertical direction (Bunnell and Vales 1990, Cook et al. 1995).

Because of the different results, Nuttle (1997) recommended that the separate concepts of "angular canopy cover" and "vertical canopy cover" should be used for different types of measurements. After a comprehensive literature review, Jennings et al. (1999) stated that the concepts "canopy cover" and "canopy closure" should have different meanings. They defined canopy cover as "the proportion of the forest floor covered by the vertical projection of the tree crowns", i.e. canopy cover should be measured in a vertical direction. On the other hand, they defined canopy closure as "the proportion of sky hemisphere obscured by vegetation when viewed from a single point". This means that if a larger area of the canopy is observed with an instrument (i.e. it has angular field of view), the result should be called canopy closure. The canopy closure is usually larger for the same stands than canopy cover: the larger the angle of view (AOV) of the observation, the larger the proportion of crowns that are viewed from the side (Fig. 1).
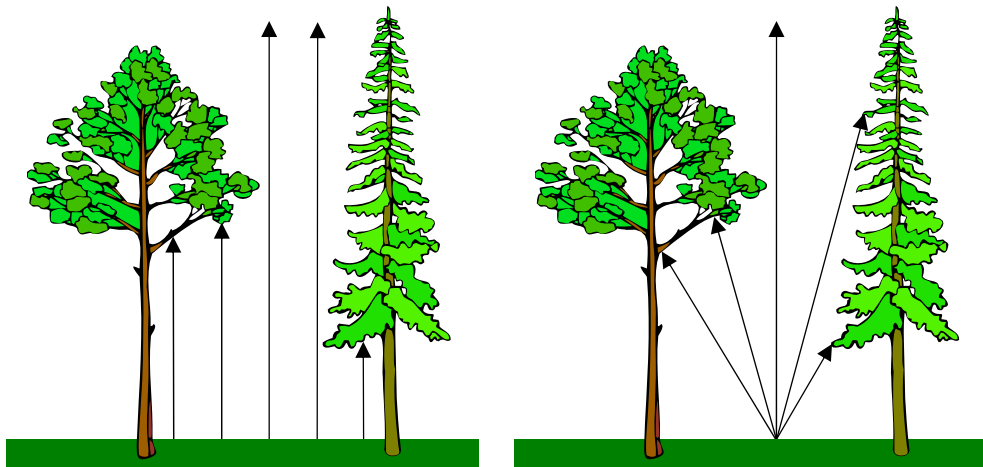
Figure 1. The difference between canopy cover (left) and canopy closure (right) is that canopy cover is measured in vertical direction and is defined for a specified area. Canopy closure is measured in perspective projection and is unique to the measured point and view angle. Image reprinted from Silva Fennica.

This division has slowly gained acceptance in the scientific community (Smith et al. 2008, Paletto and Tosi 2009), but it is not yet well known to everyone. In addition, the IPCC (2003) and the FAO (2004) state that the concepts canopy cover, crown cover, and crown closure are synonymous. Still, it would be clearer if the word "closure" was not used when referring to vertical measurements. The antonyms canopy openness and gap fraction usually include all gaps within the AOV and are thus related to canopy closure.

Common definitions of forestry concepts are particularly important for NFIs, and therefore the harmonization of concepts has been initialized. As a result, Gschwantner et al. (2009, p. 315) defined crown cover (i.e. canopy cover) through crown projection areas:

- "The crown consists of the living branches and their foliage."
- "The crown projection area of a tree is the area of the vertical projection of the outermost perimeter of the crown on the horizontal plane."
- "The aggregation of the crown projection areas of individual trees (without double-counting of overlapping crown projection areas) divided by the stand area yields the crown cover at the stand level."

The part "vertical projection of the outermost perimeter of the crown" in this definition makes several additions to the definition by Jennings et al. (1999). First, small gaps inside the crown perimeter should be classified as canopy. Secondly, dead trees and branches should be excluded. Third, if this definition is interpreted strictly, even small seedlings have crowns and should therefore be included in the CC. The first addition is important in practice, because small gaps inside the crown perimeter (Fig. 2) are usually visible in canopy photographs, and therefore must be removed from the images before CC estimation. Conversely, canopy closure, as defined by Jennings et al. (1999), has no such restrictions, i.e. canopy closure takes into account the crown transparency. The concept of "canopy cover" (CC) that is used in this thesis is, in general, equivalent to these definitions.
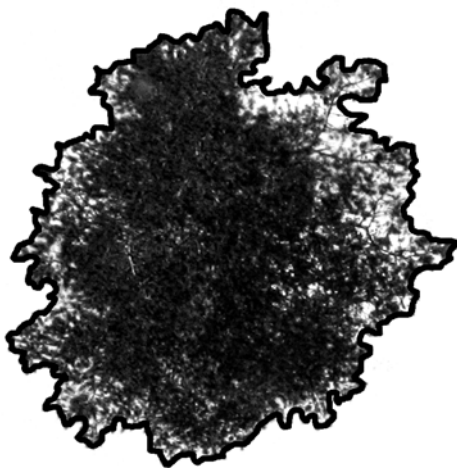
Figure 2. The outer perimeter of the crown drawn on a pine tree photographed from a helicopter. The delineation of the perimeter depends on the resolution in which the crown is observed; in the field, details smaller than 10 cm are usually ignored. The crown area determined this way is nearly always smaller than the convex hull of the crown.

1.3 Canopy cover estimation

1.3.1. Field measurements with sighting tubes

Due to the unclear definitions, there has been much uncertainty over how canopy cover field measurements should be made. If the definition by Gschwantner et al. (2010) is interpreted strictly, only vertical measurements should be accepted to obtain unbiased CC estimates. These measurements are typically made with vertically balanced sighting tubes (Sarvas 1953, Johansson 1985, Jennings et al. 1999) that do not observe the sides of the crowns. It is also easy to only record the between-crown gaps.

The Finnish version of the sighting tube is the Cajanus tube, which was named after its inventor, Werner Cajanus. Cajanus was the first professor of forest inventory at the University of Helsinki, and designed the tube in 1910's, originally for measuring crown width (Sarvas 1953, Rautiainen et al. 2005). It is a simple cylinder equipped with a mirror that allows the user to look upwards through the tube (Fig. 3). At the top of the tube is a crosshair that helps the measurement taker to determine whether the point is covered or not. The tube is attached to a holder and a support staff with a self-balancing system that makes vertical observations easy. Different versions of the same idea have been presented by several authors (Walters and Soos 1962, Bonnor 1967, Jackson and Petty 1973, Stumpf 1993).

Figure 3. Cajanus tube (photo by Pekka Voipio).

Sighting tubes can be used to measure CC in three different ways. In the dot count method (Sarvas 1953, Johansson 1985, Rautiainen et al. 2005), the area of interest is sampled with the tube. If a point is covered it is given a value of one, otherwise it is zero. The final CC is calculated as the average of the individual points. The sampling points can be located randomly, but usually a systematic sampling grid is used to guarantee coverage of the entire area of interest. This type of measurement is equal to sampling from a Bernoulli distribution, and the variance of this unbiased estimator is given by (CC(1–CC)/n), where n is the number of measurements. This formula can be used to estimate the number of sample points required for a certain level of precision, provided that the observations are uncorrelated; in case of systematic grid designs, the variance estimates may be biased because of the spatial autocorrelation between the nearby points. Based on theory and practical experience, sample sizes of 200–250 points are recommended in the literature (Sarvas 1953, Johansson 1985, Jennings et al. 1999, Rautiainen et al. 2005).

Line intersect sampling (LIS) resembles dot count sampling with predefined transects. The sighting tube and a tape measure are used to record where the canopy starts and ends above the transect, and CC is calculated as the ratio between the length of the covered transects and the full length of all transects (O'Brien 1989, Jennings et al. 1999, Williams et al. 2003). Gregoire and Valentine (2007) provided a detailed description of the error estimation and statistical background of this method.

If the tree locations at the plot are known, sighting tubes can be used to measure crown radii. With this information, an approximate map of the canopy can be drawn and CC can be estimated from the map (Lang and Kurvits 2007). Measuring more than one radius is preferable, as crowns are not typically circular. Lang and Kurvits (2007) noted that this could lead to a considerable underestimation of CC. Even with several radii, the crowns are still assumed to be convex, which is not usually true. The degree of crown overlap can also be estimated visually (Ko et al. 2009). If measured radiuses are not available, they can be modelled based on the stem diameter (see 1.3.3.).

1.3.2 Other field measurement techniques

There are also plenty of other methods that have been used in canopy cover estimation, but the sighting tubes are the most compatible with the current definition of CC as they measure the true vertical projection of the canopy. Many widely used techniques, such as canopy photography, observe the canopy using a non-zero angle of view, and are therefore better suited to measuring canopy closure. Measurements made with an AOV integrate information from different heights, and are therefore unique to the specific three-dimensional location and the AOV used. Mapping the vertical projection of the canopy this way would require that crowns were a flat 2D surface at a constant height, which is not a realistic assumption.

The advantage of AOV measurements is that the larger the area observed, the smaller the variance between individual observations at a plot. As the sample size required for a certain level of precision depends on the sample variance, AOV instruments can be used to decrease the number of sample points required compared to vertical observations. As covering an area with vertical measurements is time consuming, AOV instruments can be used to save time in CC estimation, provided that the AOV remains relatively small, within-crown gaps are correctly assessed, and the small bias in the estimate is accepted. Earlier results indicated that AOVs close to 60° (30° from zenith) produce a significant bias (Bunnell and Vales 1990, Ganey and Block 1994, Cook et al. 1995).

Traditional instruments for AOV measurements include the moosehorn (Robinson 1947, Garrison 1949) and the spherical densiometer (Lemmon 1956). The moosehorn resembles the Cajanus tube, but its shape is a pyramid or a narrow box and there is a grid of dots at the top. Canopy cover is estimated as the proportion of covered dots. The spherical densiometer (Fig. 4) is a small wooden box embedded with a convex or concave mirror. The mirror is engraved with a graticule, and the user can calculate the proportion of covered squares while looking at the reflected image of the canopy.

Another classic AOV method is the use of canopy photographs (Anderson 1964, Jennings et al. 1999, Jonckheere et al. 2005, Pekin and Macfarlane 2009). Hemispherical images are best suited for canopy closure or gap fraction estimations as the AOV is large and the resolution is also usually good enough to observe the small within-crown gaps. It is also possible to analyze just the central part of the image to reduce the AOV. If a full hemispherical view is not required, digital point-and-shoot cameras are nowadays inexpensive and easy to use for canopy photography.

Taking the photographs in the forest is quick, but getting the CC from the images requires post-processing. Typically, the images are first thresholded to separate canopy pixels from the background sky. The blue image channel is commonly used for thresholding because of the good contrast and low scattering and noise levels (Jonckheere et al. 2005, Nobis and Hunziker 2005, Cescatti 2007). The threshold can be set manually (Frazer at al. 1999) or automatically by a thresholding algorithm (Jonckheere et al. 2005, Nobis and Hunziker 2005). If CC is required, small within-crown gaps must be painted over, which can be done manually or by eliminating the gaps that are too small (Pekin and Macfarlane 2009). Finally, CC can be estimated by calculating the proportion of the canopy (black) pixels.

Figure 4. The spherical densiometer.

Angle count or relascope sampling (Bitterlich 1948, 1984) is commonly used in forestry for measuring the basal area of the stems in a stand, but it can also be used to measure the area of the crowns, and thus also CC (Bitterlich 1961, 1984). Briefly, the idea of the relascope or angle count sampling is that the basal area of the stand can be estimated by tallying the number (n) of tree stems that appear wider than the relascope's slot. The relascope function, $G = n \times BAF$, is then used to convert this number into the basal area per hectare (G). The relascope's basal area factor (BAF) (m^2 / ha) indicates how large is the increment in the basal area that each included tree represents. In Finland, the most commonly used basal area factors are one and two. Bitterlich (1961, 1984) noted that if the BAF is very large and the tree crowns are visually projected down to eye level, the crowns can be tallied similarly to the stems. For instance, if the BAF of a relascope is 200, then each crown that appears wider than the relascope's slot represents 200 m^2/ha, i.e. 2% of the hectare. Assuming that the crowns are circular in cross-section and do not overlap, each tallied crown thus adds 2% to the estimated CC. This method is especially suitable for open stands with low crowns (Bitterlich 1984).

If there are no specific instruments available or there is not enough time for actual CC measurements, ocular estimation is a commonly used option. The observer simply looks around at the plot and then gives her/his best guess of the CC. The problem is that visual assessment is extremely subjective: different observers may have different opinions of the CC at the plot. In addition, the estimation becomes more difficult if the structure of the forest is heterogeneous, or if the plot size is so large that the person must walk around to be able to assess the entire area.

1.3.3 Statistical modeling

It is often the situation that whereas standard forest characteristics are available, the CC was not estimated. In this case, models that relate CC to the known stand parameters can be utilized. If tree locations and diameters have been measured, models for crown radius (e.g. Gill et al. 2000, Bechtold 2003) can be used to create canopy maps as if the radii had been measured in the field. However, assuming that crown perimeters are circular may lead to errors (Lang and Kurvits 2007). If the tree locations are not known, they can be generated so that the degree of crown overlap can be predicted and taken into account. Often, the spatial pattern of the trees is assumed to be random (Crookston and Stage 1999), which may not always be true and thus can lead to inaccurate predictions (Christopher and Goodburn 2008). If models for typical tree patterns are available (e.g. Tomppo 1986), they can be utilized in the generation process.

Field measured CC can also be modelled directly from stand characteristics such as basal area, tree height, and stand density. Several studies have indicated that stand basal area has a strong correlation with CC or canopy closure (Kuusipalo 1985, Mitchell and Popovich 1997, Buckley et al. 1999, Vaughn and Ritchie 2005). This is easy to understand as a large stem basal area also indicates a large crown area. Stand density (stems/ha), age, height, and crown ratio have been used as additional predictors (Kuusipalo 1985, Mitchell and Popovich 1997, Knowles et al. 1999). Also, using a spatial index as a predictor could improve the results, but such information is not commonly available. On the other hand, the typical spatial structure of forests and the degree of overlap will automatically be included in the model coefficients. One important feature of a good predictor model is that the predicted CC stays at the standard unit interval [0, 1]; therefore, asymptotic nonlinear or

piecewise models are often preferred instead of simple linear regressions (Mitchell et al. 1997, Knowles et al. 1999).

1.3.4 Remote sensing

Remote sensing is the only alternative for obtaining CC information quickly for large areas. Remotely sensed images from aerial or satellite platforms are available at several scales from sub-meter to continental coverage. The classic method for CC estimation from above is the use of aerial images, which have traditionally been interpreted visually or with the help of dot count grids (Loetsch and Haller 1973, Paine and Kiser 2003). Stereo-view may also be utilized in the process (Korpela 2004, Heiskanen et al. 2008). Visual interpretation is always subjective and requires plenty of time, so calibration models may be needed (Fensham and Fairfax 2007). Thus, the focus of research has shifted toward computerized analysis of numerical aerial images. In the case of CC estimation, the most straightforward approach is the application of a segmentation algorithm to separate the crowns from their background (Culvenor 2003). For instance, in the region growing method (Wulder et al. 2000, Pitkänen 2001), the brightest pixels in the image are assumed to represent tree tops and are selected as seed points. Neighboring pixels are then iteratively added to each crown until the stop criterion is met. This is usually performed using panchromatic images or the near-infrared channel (Culvenor 2003).

High resolution aerial images are easily available for many areas, and can be acquired with relatively low costs. However, the estimation of CC from these is not without problems. First, the estimation results may depend on the scale of the images. At lower resolutions, large crowns may seem larger than they actually are (Fensham et al. 2002), while the small crowns and gaps remain unobserved (Bai et al. 2005). Second, view and illumination conditions and the spectral features of the trees vary both between and within images (Culvenor 2003). For example, in the direction of the sun the crowns seem darker because only their shadowed side is visible. In addition, the shadows may occlude smaller crowns, and also the understory may be spectrally similar to the crowns, making segmentation more difficult (Pouliot et al. 2002). These effects generally reduce the number of trees observed and they can also lead to the underestimation of crown width (Pitkänen 2001, Korpela 2004, Mäkinen et al. 2006). In the case of boreal conifer forests, some of these problems can be avoided by using images taken during annual snow cover (Manninen et al. 2009). Even if these issues can be accounted for, the problem of the relief displacement effect (Mikhail et al. 2001) remains: if the plot is not located directly at nadir, sides of the crowns are seen as well, exactly as with ground-based AOV instruments. Thus, estimates obtained from aerial images may be biased even if the crowns can be segmented correctly, but empirical models can be used for calibration (Mäkinen et al. 2006). A better approach could be the utilization of photogrammetric multi-image matching methods to create canopy surface models directly from overlapping aerial image data (Hirschmugl 2008), but the precision of this approach in crown width detection has not been tested.

High resolution satellite images (e.g. Ikonos, Quickbird) also enable the detection of individual crowns (Palace et al. 2007, Song et al. 2010, Chopping 2011). Canopy cover can also be modelled directly based on the spectral and spatial features of the image (Chubey et al. 2006). The advantage of the satellite over aerial images is that the effect of relief displacement is considerably smaller. Nevertheless, in Finland, these data are not commonly used because the availability of images is often limited due to cloudy weather

and the small coverage of individual images. Also, the costs are often considerably higher than with aerial images.

Medium resolution (typically 5–30 m) sensors carried by different Landsat and SPOT satellites, for example, observe the Earth at several spectral bands ranging from visible blue to middle infrared. At these resolutions, individual tree crowns can no longer be distinguished, but CC can still be estimated using either an empirical or a physical approach. In the empirical approach, statistical models are used to link the field-measured reference data with the observed reflectances. Different indices describing the vegetation can be derived by combining two or more spectral bands; for instance, the commonly used NDVI (normalized difference vegetation index) is based on the red and near-infrared bands (Lillesand et al. 2004). The models can then be used to predict CC and other parameters for the whole image (e.g. Carreiras et al. 2006, Wolter et al. 2009). Empirical methods are also used for global forest area monitoring with low resolution (>100 m) satellite imagery (Hansen et al. 2003).

The physical approach to satellite image interpretation is based on mathematical modeling of the transfer of solar radiation in the vegetation. These reflectance models can then be inverted in order to deduce biophysical properties of the forest canopy (such as CC and leaf area index) from the reflectances observed by the sensor (Liang 2004, Stenberg et al. 2008). The difficulty is that many physical models require simplifying assumptions of the forest structure, and the required *a priori* data may not always be available (Stenberg et al. 2008). In structurally complex boreal forests where the foliage and the background may have relatively similar reflectances, the plot-level CC estimation is a very difficult problem (Gemmell 1999, Gemmell and Varjo 1999, Gemmell et al. 2002). Nevertheless, physical models have been used for CC estimation more successfully in other biomes (e.g. Jasinski 1996, Woodcock et al. 1997, Zeng et al. 2009).

Active remote sensing sensors, including radars (radio detection and ranging) and LiDARs (light detection and ranging), emit electromagnetic radiation and record the properties and location of the backscattered signal, which can then be linked to forest characteristics. Radars emit microwave radiation (wavelengths approximately 0.001–1 m) that penetrates the atmosphere in practically all conditions (Lillesand and Kiefer 2004). Side-looking radars can produce images at several bands, and these features can be empirically linked to the measured forest parameters, such as height, volume, and leaf area index (e.g. Manninen et al. 2005, Holopainen et al. 2010). However, at least in Finland, imaging radars have not been used in practical forest inventories because the reflected radar signal is sensitive to soil moisture and metal objects (e.g. powerlines), for example, and the signal is noisy at plot level (Lillesand and Kiefer 2004). Profiling radars produce forest height observations directly under the platform, and thus enable the estimation of forest cover (e.g. Hyyppä and Hallikainen 1996). However, covering large areas by vertical measurement is very expensive. The precision of radars against detailed *in situ* CC data has not been tested so far.

Many of the difficulties related to radar systems can be overcome by using laser beams at near-infrared wavelengths (commonly 1064 nm) instead of microwaves. These LiDAR sensors come in different types and may be placed on any platform, but in forestry the most commonly used systems are discrete return scanning LiDARs that are meant for topographic mapping from aerial platforms (Næsset et al. 2004). The laser scanner is mounted on an aircraft, which also carries a GPS and an inertial measurement unit that are used to record the position and orientation of the aircraft. The scanner emits laser pulses and records the time it takes for the echoes (typically 1–4) to return, so that the distance can

be calculated. During post-processing, the differentially corrected GPS data are combined with scanner orientation data so that a georeferenced point cloud is created (Wehr and Lohr 1999). In the case of forests, some fraction of the echoes originates from the trees and the rest from the ground. Thus, the ground echoes must be recognized first so that a digital terrain model can be interpolated (e.g. Axelsson 2000). The Z coordinates of the echoes can then be normalized into heights above ground level.

Different coverage metrics for the area of interest can be easily calculated from this type of data. A simple estimate of CC can be obtained by first deciding a threshold height (e.g. 1.3 m) and then calculating the fraction of first returns above this threshold (e.g. Lovell et al. 2003, Rianõ et al. 2004, Morsdorf et al. 2006, Holmgren et al. 2008). As the typical off-nadir angles of the laser pulses are small (usually less than 20°), this index resembles dot count measurement with a sighting tube. Nevertheless the pulses are not exactly vertical, so a small overestimation is likely as the oblique pulses have a smaller probability of reaching the ground than vertical ones (Holmgren et al. 2003). Thus, regression calibration with field-measured CC may be necessary (Holmgren et al. 2008). Airborne LiDAR data are considered to be so accurate that validation results may sometimes tell more of the quality of the field data than the precision of the LiDAR estimates (Smith et al. 2009).

Terrestrial LiDARs (TLS, terrestrial laser scanning) can also be used for a detailed characterization of the forest canopy structure, including CC measurements (Danson et al. 2007, Jupp et al. 2009, Korhonen et al. 2010). These LiDARs are mounted on a tripod and scan the surroundings in a hemispherical field of view, producing a 3D point cloud of the surroundings. Because of the view geometry, the TLS systems are better suited for measuring canopy closure or the conical gap fraction. The angular effect can be eliminated by creating canopy maps, which can be done, for example, by calculating the density of canopy echoes in a 2D grid (Korhonen et al. 2010). The number of scan locations must, however, be reasonably large to cover the entire plot, as most of the pulses will reflect from the nearest crowns.

1.4 Objectives

In Finland, the traditional method used in canopy cover estimation is systematic dot count sampling with the Cajanus tube (Sarvas 1953). This method yields accurate results and has a solid statistical background (Jennings et al. 1999, Rautiainen et al. 2005), but the measurements are too slow for inventories where the time available for CC estimation is at best a few minutes. Thus, the main objective of this thesis was to test various alternative CC estimation techniques, including quicker field measurement techniques, statistical models based on standard forest inventory parameters, and remote sensing with airborne LiDARs. Different field measurement techniques produce different estimates of CC, mainly because of differences in view geometry and crown transparency. The degree of these effects on the estimated CC was therefore examined.

This thesis consists of five sub-studies. Study I introduces the terminology and field control method, and it also tests some of the commonly used fast ground measurement methods. Study II extends the first study by presenting a regression model for CC using the data from the same research area, and discusses its application. Study III introduces a modified version of the standard relascope, the crown relascope, and tests its usefulness in CC measurements. Study IV describes an automated method for analyzing digital canopy images and examines the effects of the different AOVs on the estimated CC. Finally, study

V tests the precision of airborne laser scanning in CC estimation and the methods for normalizing the effect of oblique laser pulses. This summary also includes some yet unpublished material, such as the nationwide version of the CC model introduced in study II.

2 MATERIALS AND METHODS

2.1 Research areas

The research data, in total 263 plots with CC measurements, were gathered from several study sites in different parts of Finland (Table 1, Fig. 5). Most of the Finnish forests are managed for timber production, and especially in Southern Finland natural stands are rare outside nature reserves. The forests are usually harvested by clear or seed tree cutting, after which the clearings can be regenerated naturally, by seeding, or by planting, usually after soil preparation. The publicly recommended forest management scheme includes several thinnings during the rotation (60–120 years), but in practice the intensity of management depends on the forest owner, as most of the forested area is owned by individual citizens. The dominant species are usually Scots pine (*Pinus sylvestris* L.), Norway spruce (*Picea abies* L. *Karst*), or birches (*Betula spp.* L.). A few stands dominated by European aspen (*Populus tremula* L.) were also included. In Northern Finland, the climate gets colder and stand densities and tree heights decrease, which also mean smaller CC.

The plots were usually located subjectively so that as diverse a data set as possible was obtained from each study area, and as a whole. The structural variation included different dominant species and site types, tree heights, stand densities and CCs. Thus the final data included everything from low CC seedling stands and sparsely wooded pine bogs to dense young forests and natural old-growth stands with high CC. Canopy cover was measured at each plot using the Cajanus tube (see 2.2.) and also usually with other methods for comparison.

Subsets of the whole data were used in the sub-studies. In study I, the data consisted of a subset of 19 plots in Suonenjoki, where several field measurement techniques were compared. The original measurement plot type in Suonenjoki was a 25 × 24 m rectangle, but in the analysis phase the size of the plot was decreased to a circle with a 12.5 m radius for a better correspondence with the Finnish NFI. Study II, which focused on CC modeling, included all of the 100 plots from the Suonenjoki site for the model construction, and 30 plots from the Koli site for testing. The empirical part of study III, in which the crown relascope was tested, was based on all of the available circular plots in the northernmost part of Finland (7 at the Rovaniemi and 66 at the Sodankylä sites), where the relatively low tree densities favored this measurement technique. Study IV focused on automated canopy image analysis, and the data consisted of all plots where the trees had reached a minimum height of 5 m at the Koli (n=29), Tammela (n=5), Joensuu (n=5), Rovaniemi (n=3) and Sodankylä (n=53) sites. Finally, the LiDAR-based CC estimation in study V was tested at the rectangular plots at Koli (n=30) and Hyytiälä (n=22).

Table 1. Study sites.

	Year	n	Size (m)[a]	Studies	Methods
Suonenjoki[b]	2005-2006	100	25x24	I, II	Camera, densiometer, ocular
Koli	2006	30	30x30	II, IV, V	Camera, LiDAR
Tammela	2007	7	r=12.5	IV	Camera, ocular
Joensuu	2007	8	r=12.5	IV	Camera, ocular
Rovaniemi	2007	7	r=12.5	III, IV	Camera, crown relascope, ocular
Sodankylä	2007	68	r=12.5	III, IV	Camera, crown relascope
Evo	2008	4	r=12.5		
Paltamo	2008	3	r=12.5		
Hyytiälä	2008	24	Variable	V	LiDAR
Sotkamo	2009	12	r=12.5		
Matalansalo[c]	2004	472	r=9.0		LiDAR

[a]Plot size most commonly used in the area. Rectangular dimensions or radius are given.
[b]Divided into two sub-sites, Hirsikangas and Saarinen
[c]No *in situ* CC measurements, LiDAR data used for model tests.

Figure 5. Locations of the different study sites.

Table 2. Summary of the whole data set (263 plots) and separately for each dominant species (Scots pine 145 plots, Norway spruce 97 plots, deciduous species 21 plots).

		Min	Mean	Max	Sd
Canopy cover (%)	Pine	2.2	50.7	96.5	21.8
	Spruce	16.6	67.8	96.8	17.2
	Deciduous	2.4	75.4	97.5	23.7
	All	2.2	59	97.5	22.4
Basal area (m^3/ha)	Pine	0.0	16.5	54.1	10.5
	Spruce	1.0	22.5	49.7	10.2
	Deciduous	0.0	20.1	36.8	12.4
	All	0.0	19.0	54.1	10.9
Stand density (stems/ha)	Pine	95	2400	12500	2230
	Spruce	383	2500	15900	2210
	Deciduous	250	3500	17100	3930
	All	95	2520	17100	2410
Stem diameter (cm)	Pine	0.0	17.5	41.7	10.2
	Spruce	2.9	19.8	66.5	10.3
	Deciduous	0.0	17.3	37.9	11.2
	All	0.0	18.3	66.5	10.3
Tree height (m)	Pine	0.4	13.7	32.6	7.4
	Spruce	2.9	16.3	35.5	7.0
	Deciduous	0.4	15.7	28.0	8.7
	All	0.4	14.8	35.5	7.4

The combined data of 263 plots were also used together in making the nationwide CC model, first published in this thesis summary. Table 2 displays the main stand characteristics for the combined data set. The nationwide model was tested by predicting the CC for the 472 sample plots at the Matalansalo (62° 18'N, 28° 29' E) LiDAR study site, located 70 km southeast from Joensuu (Suvanto and Maltamo 2010), and by comparing the results to LiDAR-based estimates.

2.2 Canopy cover field control measurements

Reliable CC control data is the basis for the results presented in this thesis. Following the definitions presented in section 1.2, reliable estimates of the vertical CC can only be obtained by covering the entire plot with unbiased vertical measurements. Based on earlier experience (Sarvas 1953, Johansson 1985, Rautiainen et al. 2005) and compatibility with the CC definition, the classic, systematic dot count sampling with the Cajanus tube was selected as the control method for studies I–II. In practice, the field protocol first included establishing the parallel sampling transects, which were located at a 2.5 m distance from each other in studies I–II (Suonenjoki and Koli sites). Transects were marked with a tape measure which allowed objective determination of the sample points. The measurements were taken by walking along each transect and looking up through the tube at 1 m intervals. If the crosshair at the top of the tube pointed at a crown (or a small gap inside the crown),

"1" was saved into the spreadsheet on the handheld computer, otherwise "0". The density of the crown above the sample point had no effect, just the location of the point inside or outside of the crown perimeter mattered. After the plot was finished, the handheld computer showed the resulting CC directly.

Deciding whether the point was covered or not sometimes required subjective consideration. If the crosshair was pointed exactly at the edge of the crown perimeter, or if the crown was moving slightly because of the wind, a decision was made based on the full field-of-view of the tube (a few degrees). If that was impossible, every second controversial point was classified as canopy. In a strong wind the mensuration became impossible if the crowns were moving continuously. Also, the rain effectively stopped the measurements as moisture blurs the mirror inside the tube, even if the water is wiped from the top. The measurement in itself was reasonably fast, especially when clearly covered or open points could be recorded without using the tube. However, placing the tape measures along the transects could take even longer than the actual measurement, depending on the terrain.

Small seedlings and young stands where the living base of the crown might have been below eye level (1.7 m, the height of the tube's crosshair) required some additional consideration. When interpreting the definition by Gschwantner et al. (2009) strictly, small seedlings should also be included in CC. Also, larger tree crowns can reach a sample point lower than eye level. In these cases the support staff was used to determine the coverage. The height threshold used to divide the covered points into "understory canopy" and "actual canopy" was 1.3 m, as this was the height where, for example, the canopy photographs were taken. If the point was covered below 1.3 m, it was saved into the spreadsheet with the letter "u" (seedling smaller than 1.3 m) or "a" (tree taller than 1.3 m but the crown only reaches the sample point below 1.3 m). These letters could be afterwards converted to either 1 or 0, depending on whether total cover or cover above 1.3 m was required. Dead trees and branches created a similar problem. According to the definition (Gschwantner et al. 2009), they should not be included in CC, as a crown should only include living branches and their foliage. Thus, single dead twigs, branches and snags were ignored, but if they covered a significant portion of the tube's field of view (e.g. if the point was right under a dead spruce tree), the point was labeled with "k", which could be classified as covered if necessary.

The dot count measurements were taken in the Suonenjoki and Koli research sites, which were used in studies I-II. Starting from 2007 (studies III–V), the control measurement scheme changed so that line intersect sampling (LIS) (O'Brien 1989, Gregoire and Valentine 2007) replaced the dot counts. Now the tube was used to measure all start- and end-points of the canopy above the measuring tape, and the results were recorded to 10 cm precision. This way more precise results could be obtained, especially in low cover stands where the 1 m dot interval could not always detect small crown intersections. However, the disadvantage of the LIS method was that measuring became very slow in stands with a lot of small intersecting crowns. On the other hand, if the number of the crown edges was small, for instance in stands with big crowns or a very dense canopy, LIS could be even faster than the dot count. The LIS transect interval was 3.0 or 2.5 m, depending on the plot size.

Yet another method of obtaining the field control was tested at eight plots in the Hyytiälä site (study V). The tree positions at the plots had been measured in advance using a photogrammetric-geodetic method (Korpela et al. 2007), so the Cajanus tube was used with a laser rangefinder to measure crown radii in four perpendicular directions per tree. Subsequently, a computer script was used to calculate the CC from the known tree locations

and radius measurements by modeling the crowns as four quarter-ellipses. This was done by using a 10 cm grid for each plot and by performing an inclusion test for each grid cell. Furthermore, trees in the buffer zone outside the plot borders were also measured as their crowns often reached into the plot.

All control measurements were taken by the author. Thus, the results could have been slightly different if someone else had taken the control measurements, as the decisions of the crown edges involved some subjectivity. In the existing studies, no significant differences were found between measurement takers (Johansson 1985, Vales and Bunnell 1988). During the field campaigns, individual transects were duplicated a few times by a less experienced person. The differences did not exceed 5% in these tests. Possible problems can in most cases be avoided by giving detailed instructions on how to act in unclear situations (Johansson 1985, Vales and Bunnell 1988, O'Brien 1989).

2.3 Tests of the different field measurement techniques

2.3.1 Different sampling densities with the Cajanus tube

The mensuration of control values with the Cajanus tube is considered reliable, but with the tested sampling schemes the measurements usually took more than an hour, even in structurally easy plots. Thus, in study I, we tested how the reduction of sampling density affected the estimation of CC using the tube. In practice, this was done be removing every second, fourth and eighth point out of the original 195 samples, leading to densities of 102, 49, and 23 points per plot, respectively. In addition, the sampling transects were measured using both the dot count and LIS methods so that the differences in results could be compared.

2.3.2 Spherical densiometer

The spherical densiometer (Lemmon 1956) was tested as a traditional AOV method. The instrument (Fig. 4.) is used by counting canopy proportions within each cell in the grid engraved on the mirror. However, earlier studies indicated that using the whole grid (60° AOV) would lead to a significant overestimation of CC (Bunnell and Vales 1990, Ganey and Block 1994, Cook et al. 1995), so the sampled AOV was reduced to about 20° by using just the four squares that reflected the canopy directly above the measurement point. In study I, the densiometer was used to sample 49 points from the Cajanus tube grid (every fourth point), and this sample was further reduced to 23 and 9 points per plot. In addition, subjective sampling was tested: the measurement taker selected ten representative points and measured them with the instrument.

The original data in study I included four seedling stands (the largest had a mean height of 6.2 m) where the densiometer and camera methods did not produce good results. The reason was that the Cajanus tube was also used to record the twigs below breast height if the tree was taller than 1.3 m, whereas both the densiometer and camera were held at breast height. The AOV methods are useful only in sites where the bases of the crowns lie well above the measurement height. Thus, in this summary the seedling stands were removed from the study I densiometer and camera results in order to give a more realistic view of the results in real situations.

2.3.3 Digital cameras

Compared to the spherical densiometer, the use of point-and-shoot digital cameras facilitates the field measurement by removing the error-prone grid cell tallying. Instead, the canopy image is saved as a document for further analysis. In study I at Suonenjoki, a digital camera was used to take five images from each plot: one at the center and the other four at cardinal points at an 8.5 m distance from the center. This sampling scheme had been used in some earlier tests related to the Finnish NFI. The AOV of the camera (Kodak DC4800) was approximately $63 \times 49°$, which was already so large that a significant bias could occur (Bunnell and Vales 1990, Ganey and Block 1994, Cook et al. 1995).

The images were then analyzed manually with Paint Shop Pro software by first thresholding them manually. The threshold was set by the interpreter so that the classification of sky and canopy pixels would correspond to the original image as well as possible. The proportion of black pixels in the binary images could then be calculated from the image histogram. However, these results were in fact estimates of canopy closure, as the small within-crown gaps were still visible. Thus, standard tools were used to paint over the crowns with a black color, so that the crowns became opaque. Both painted and non-painted images were, nevertheless, included in the analysis in study I.

The manual post-processing described above was rather laborious. The interpreter had to manually select a threshold value for each image, which could lead to inconsistent results (Jennings et al. 1999, Jonckheere et al. 2005, Nobis and Hunziker 2005). In addition, the painting of the within-crown gaps had to be done carefully. However, these phases can be automated, as is demonstrated in study IV using the Matlab numerical computing environment (MathWorks Inc. 2008). The images were first thresholded using the automated algorithm by Nobis and Hunziker (2005) with just the blue RGB component (Jonckheere et al. 2005, Nobis and Hunziker 2005, Cescatti 2007). The algorithm selects the threshold that maximizes the mean brightness difference between the pixels on the crown and sky sides of the edges (Fig. 6).

The crowns in the resulting binary images must yet be painted opaque so that only the between-crown gaps are visible in the final version. This was done automatically using morphological image analysis operations (Gonzalez and Woods 2002, pp. 523–527). The morphological dilation and erosion are based on the use of a moving window, which, in this context, is called the "structuring element". In the dilation of a binary (1/0) image, the structuring element is moved through the image and if there is at least one value of "1" inside it, the pixel that is tested is also marked as "1". Thus, dilation expands objects and fills gaps. Its opposite, erosion, labels the pixel of interest "0" if at least one "0" is present within the structuring element. As a result, erosion shrinks objects and expands the gaps.

In the crown painting algorithm, the thresholded image is first dilated, then eroded twice, and finally dilated once more with the same structuring element. The first dilation followed by erosion is commonly called morphological closing, an operation that removes the small gaps within the crowns. The next erosion followed by dilation can correspondingly be called morphological opening; this operation is used to smooth the final image by eliminating the unnecessary details introduced in the closing (Gonzalez and Woods 2002). The structuring element used to perform these operations was disc-shaped to increase the smoothness of the crown perimeters. The final image showed only the large between-crown gaps, where CC could be estimated as the percentage of black pixels (Fig. 6).
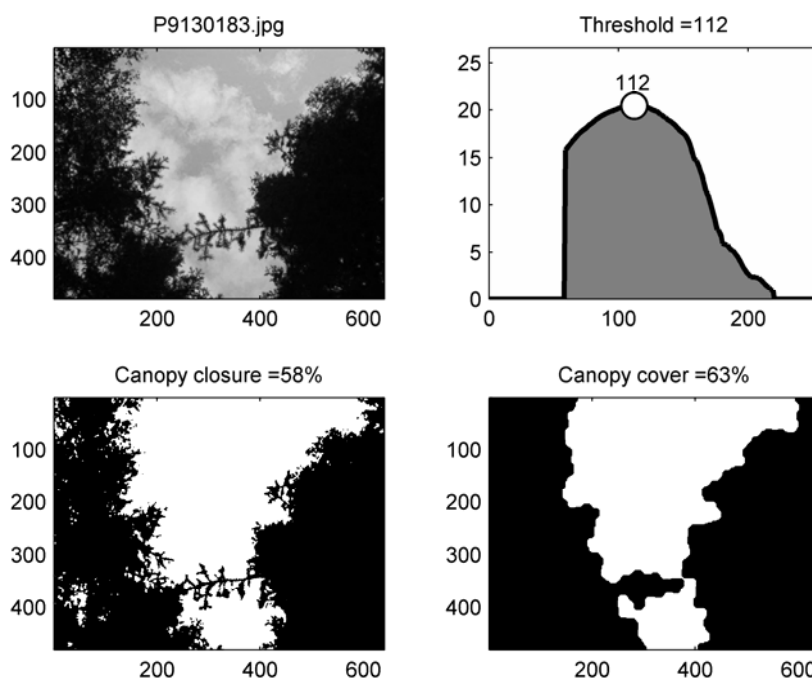
Figure 6. Automated canopy image analysis. The upper-left image shows the original blue channel. The upper-right graph shows the mean brightness difference at each possible 8-bit brightness threshold. The lower-left image shows the result of thresholding, and in the lower-right image the crowns were painted black using the morphological method so that just the between-crown gaps are visible.

The image processing chain was first validated by comparing the CCs derived manually and the automatically analyzed images from the Koli site. Then, just the automated processing was used to estimate CC for the rest of the data, and, finally, the results were compared to the Cajanus tube estimates. In study I, the whole rectangular image area was considered, but in study IV, a circular area determined by the given AOV was used instead. In addition, the effect of different AOVs was tested by decreasing the size of analyzed area. Different point-and-shoot cameras were used in the field, but the image resolution was kept at the minimum 640 × 480 pixels, which sufficed for determination of the large between-crown gaps. The number of images required for reliable estimates at plot level was also estimated based on the variance between the images.

2.3.4 Crown relascope

Walter Bitterlich's original idea of measuring crowns with relascopes (Bitterlich 1961) was based on the visual projection of the crown width to eye level. The visual part can be avoided if the entire crown can be seen through the relascope's slot, i.e. the slot must be very high and wide. In study III, we presented the crown relascope, which is suitable for this type of measurement. The first prototypes had a solid distance stick and a fork-shaped

slot, but this design was soon found to be rather cumbersome. Thus, the slot was replaced by a long plastic sheet and the stick with a short string to increase portability (Fig. 7).

The problem with crown relascope measurements is that the height at which the largest crown width occurs is not constant, and therefore the relascope's slot must be very high. Because of this, the BAF must be defined slightly differently for the crown relascope. Normally, a stem is tallied if its convex closure appears wider than the relascope's slot, i.e. the real stem width cannot be seen from a close distance. As the stem intersections are assumed to be circular, this does not matter as the crown radius is related to the sine of the relascope's half angle and the tree's distance (Bitterlich 1984). But in three dimensions, the circularity assumption should be generalized to spherical crown shape, which is not realistic. This can be avoided by changing the definition of BAF so that instead of the visible crown width, the true crown width perpendicular to the look direction should be sighted. The BAF would thus be based on the tangent instead of the sine. Thus, it is better to use separate concept CBAF (crown basal area factor) for the crown relascope. For example, a cylindrical crown near the measurement taker must be measured at a very steep angle. The apparent crown width, or the width of the crown's convex closure, is larger near the base of the crown because the distance to the eye is smaller. The true crown width is constant, so the observer must ignore the branches reaching slightly towards her/him, and make the inclusion decision based on perpendicular branches. Whilst this is not possible for opaque objects such as stems, it is for transparent crowns, although careful consideration is required during the measurement.
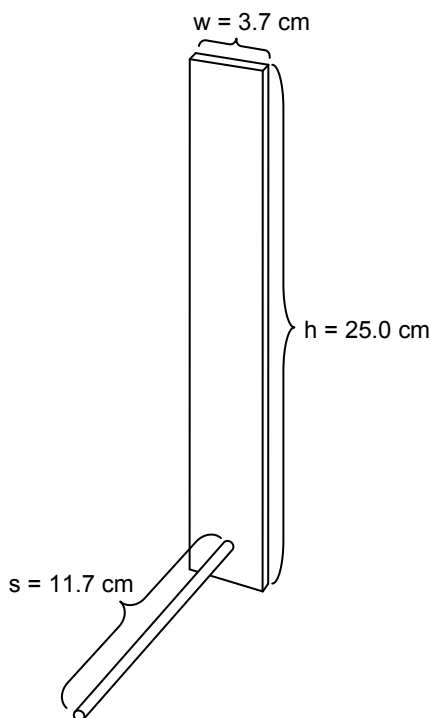

Figure 7. The design of a crown relascope with a basal area factor of 250. Image reprinted from Canadian Journal of Forest Research.

In practice, the effect of the CBAF definition on CC estimation is small compared to other error sources. One practical problem is that the crown intersections are still assumed to be circular, which is not true, as the real crown area is practically always smaller than the area of a circle drawn around it. Another assumption is that the crowns do not overlap. If these assumptions are not met, CC will be overestimated. The more distant crowns may remain partially or totally occluded, so the measurement taker must be very precise in observing everything. In order to keep the measurement accurate, the relascope's slot must be kept vertical and the distance stick horizontal, which further increases the challenge.

In study III, a sheet-and-string crown relascope with CBAF=250 was tested at the two northernmost study sites, Rovaniemi and Sodankylä. This region is well suited for crown relascope measurements as the tree densities are usually low and crown overlap is not too common. The CBAF of 250 was chosen as a compromise – smaller CBAFs such as 100 would lead to more accurate results in sites with a low tree density, but in a forest with 60% CC, for example, the tally should include 60 trees, which is quite a large number. On the other hand, larger CBAFs do not necessarily represent the whole plot if the crowns are not very wide. In study III, the crown relascope was used at every plot without considering whether the plot was actually suitable for this measurement (good visibility, small overlap); with a stricter stand selection, better results could have been obtained.

2.3.5 Ocular estimation

Ocular estimation is the simplest method for making *in situ* CC estimates. In study I, the ocular estimates were made by three people: the author and two Finnish NFI group leaders who had been making this kind of estimation in practice. The author made the estimations before measuring the stand with a Cajanus tube, and thus had a chance to learn from the earlier plots. Before the test, the group leaders were told to make the estimations as they had done before the test during the summer's NFI, i.e. no instructions were given.

Another previously unreported test was performed in spring 2007 during the Finnish NFI training days at the Tammela, Joensuu and Rovaniemi sites. The group leaders who were responsible for making the CC estimations were given instructions on how CC is defined and which things should be considered during the assessment. They recorded the estimates at each plot before the Cajanus tube CC was given. This way, they could learn from the earlier plots and calibrate their eyes for the next summer's campaign.

2.4 Statistical canopy cover models

The aim of study II was to model CC based on the forest characteristics that are commonly available at forestry stand registers, such as basal area, tree height, diameter at breast height, site index, and species proportions, and so forth. The tree locations and other metrics describing the spatial tree pattern are not usually available, so this work focused on the direct utilization of correlations linking the CC to the known inputs.

In case of CC modeling, the dependent variable is a percentage. This creates two possible difficulties if simple linear regression is used. First, the model may produce estimates that are outside the standard unit interval [0, 1]. Secondly, when percentage variables are predicted, the error distributions are often asymmetric (Ferrari and Cribari-

Neto 2004), which contradicts the residual normality assumption of the linear regression analysis. Thus, instead of the normal linear regression, a relatively new modeling technique called beta regression (Ferrari and Cribari-Neto 2004) was introduced in study II for CC modeling.

The beta regression method is an extension of the generalized linear models (GLMs) (McCullagh and Nelder 1989), and it is especially meant for modeling rates and proportions. The GLMs differ from the standard linear regression in that the expected values μ_i of the random variable Y are replaced by a link function $g(\mu_i) = \eta$, where η is a linear combination of the predictor variables. The purpose of the link function is to stabilize the error variance and transform the fitted values to the desired application range. In addition, the error distribution of the model can be chosen independently, whereas in linear regression the error distribution is always assumed to be normal.

In the beta regression, the residuals are assumed to follow a beta distribution, which is a better assumption than the usual residual normality. In percentage modeling, the link function must be chosen so that it is asymptotic at both ends so that the model does not produce irrational estimates. Several asymptotic link functions can be used for beta regression, but the logistic link function was chosen in study II (Eq. 1) (McCullagh and Nelder 1989, p. 108):

$$\log(\frac{\mu}{1-\mu}) = \eta = \sum_{j=1}^{p} x_j \beta_j \tag{1}$$

where μ = predicted canopy cover, η = linear combination of predictor variables, x_j = vector of predictor variables, and β_j = vector of model coefficients. The predicted values were obtained as the inverse of the logistic function (Eq. 2):

$$\mu = \frac{\exp(\eta)}{1 + \exp(\eta)} \tag{2}$$

The model parameters were estimated using the maximum likelihood method in the R statistical computing environment (R Development Core Team 2008), with an additional betareg library. The estimation procedure is slightly different from the standard GLM estimation since the beta distribution does not belong to the exponential family (Ferrari and Cribari-Neto 2004).

In study II, local CC models for Scots pine (n=52) and Norway spruce (n=48) dominated plots were constructed with the beta regression technique using the data from the Suonenjoki research site. Coefficients of determination, standard errors, residual plots and Akaike Information Criterion (AIC) (Sakamoto et al. 1986) were used for a comparison of model performance. The models were cross-validated by randomly removing ten (pine data) or nine (spruce data) plots from the base data and refitting the model with the remaining plots, which was repeated a hundred times for each model.

A combined data set of 263 plots was used to make nationwide versions of the local models presented in study II. As the modeling data were from different parts of Finland, north coordinate was introduced as an additional predictor. Because the number of plots dominated by the deciduous species was small (n=21), the deciduous stands were included in the Norway spruce model and the proportion of the deciduous trees in the basal area was used as an additional predictor. Site quality was described by dummy variables representing

different taxation classes (Valtakunnan metsien… 2008). These models were also cross-validated and, in addition, the model predictions were compared to the CC estimated from the airborne LiDAR data at the Matalansalo site (see 2.6).

2.5 Airborne laser scanning

The use of airborne laser scanning in CC estimation was tested in study V. Several LiDAR data sets were available from the Koli and Hyytiälä study sites, but in this summary just the main results from the Koli 2005 and Hyytiälä 2007 and 2008 1 km scans (Table 3) are discussed. For the Koli site, all of the 30 rectangular sample plots that were measured in spring 2006 were included in the scanned area. For the Hyytiälä site, 22 rectangular sample plots were covered. Both the Hyytiälä 2007 scan and the Koli scan were flown with fairly similar acquisition settings, so that the pulse density was high enough to recognize individual trees (4.6–10.3 pulses per m^2). The Hyytiälä 2008 1 km scan differed from the normal forestry scanning set-up in that the half scan angle was exceptionally high, at 32.5°.

Several different approaches for obtaining the CC from the LiDAR data were tested. In all cases, only the single and first-of-many echoes were used, as they included all of the information required for CC studies (Morsdorf et al. 2006). The simplest of the test techniques was to calculate the proportion of canopy echoes above the 1.3 m height threshold. In study V, this index was labeled as the FCI (First echo Cover Index) to separate it from the other indices that included other echo types. This index was then compared to the Cajanus tube reference (where the canopy elements below 1.3 m were ignored) using all of the available date sets.

The problem with the scanning LiDAR is that most of the pulses emitted are not exactly vertical, which may lead to a slight overestimation of CC. This happens because the pulses arriving at an oblique angle have a larger likelihood of hitting a crown than vertical ones. Holmgren et al. (2003) proposed several methods that could be used to decrease this bias. The first alternative is to just use the vertical echoes. We evaluated this approach by using only the echoes from the nearest strip. Another alternative is to make linear regression models where the scan zenith angle and other LiDAR-derived variables are used to predict the bias in the estimated CC. This was tested with the Hyytiälä LiDAR data, where mean scan zenith angles were calculated for each plot and scan strip.

Table 3. The most important airborne LiDAR data sets used in study V and their acquisition parameters. Both scanners operated at a 1064 nm wavelength.

	Koli 2005 1 km	Hyytiälä 2007 1 km	Hyytiälä 2008 1 km
Date	July 13	July 4	August 23
Sensor	ALTM 3100	ALS50-II	ALS50-II
Mean range, m	950	780	960
Half scan angle	11°	15°	32.5°
Mean pulse density m^{-1}	4.6	10.3	2.7
Mean footprint diameter, cm	29	12	14
Pulse frequency, kHz	100	115.8	92
Scan frequency, Hz	70	52	35
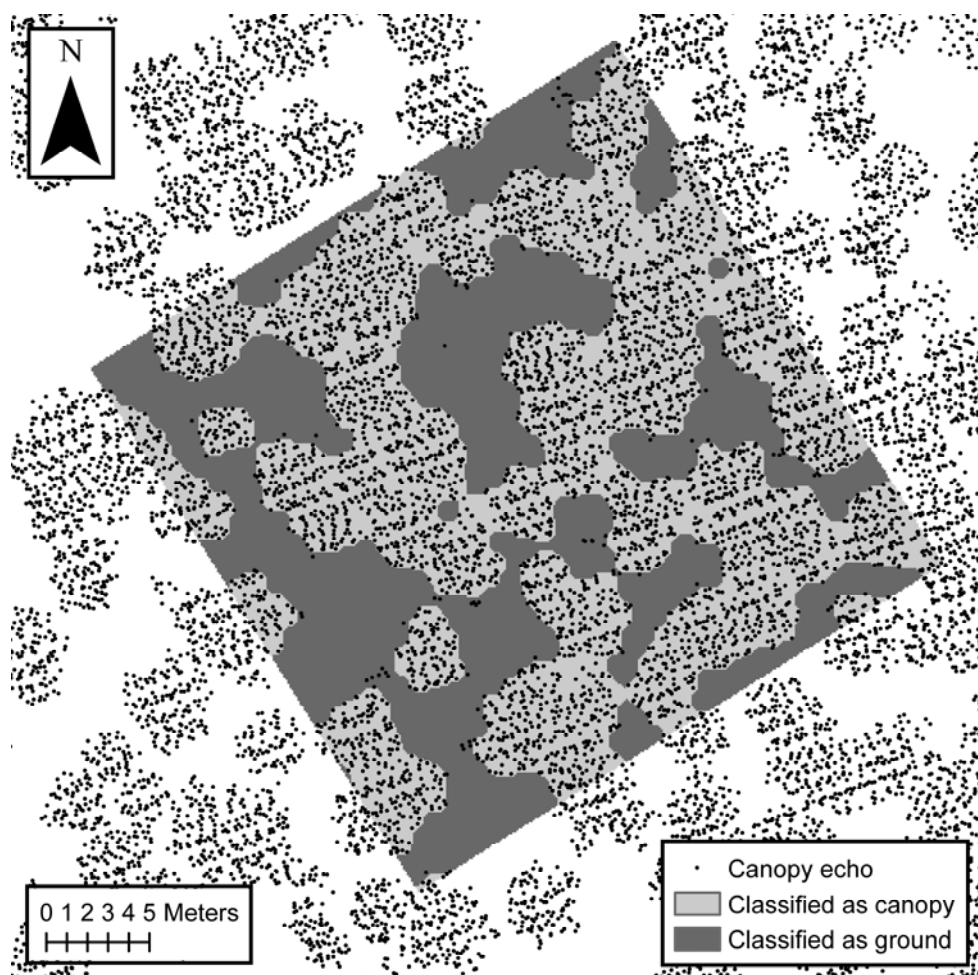
Figure 8. A canopy map derived from airborne LiDAR data using morphological image analysis.

One way of decreasing the overestimation is to allocate the laser echoes to a grid and to use the grid in the CC calculations instead of using the echoes directly. As the oblique pulses tend to gather on the crowns, selecting just one echo from each grid cell typically increases the proportion of ground echoes and thus decreases the overestimation. The first of the grid-based methods to be tested was where a random echo was selected to represent each cell and then the FCI was calculated from the selected echoes. This approach is similar to the data decimation technique by Vauhkonen et al. (2008). An alternative method is to select the highest echo from each cell. The mapping of maximum cell heights leads to the commonly used canopy height model (CHM) method (Hyyppä et al. 2001). The CHM can be used for mapping the location of canopy gaps, as well as for estimating CC.

Canopy maps of a finer resolution can be derived by using morphological image analysis (Wang et al. 2008). In this approach, the morphological dilation and erosion operations (Gonzalez and Woods 2002) are used to fill the gaps in the sparsely populated

initial canopy map, exactly as was done for the thresholded canopy images (see 2.3.3.). The only difference is that the within-crown gaps are now empty pixels between the cells that had canopy echoes. In study V, the echoes were allocated to a 0.1 m resolution grid, which was then processed with the morphological closing and opening operations. The final map (Fig. 8) shows which parts of the plot are covered by the canopy.

2.6 Comparison of the nationwide model estimates to airborne LiDAR data

The nationwide CC models were tested by predicting the CC for the data set containing 472 plots collected from the Matalansalo LiDAR study site. The Matalansalo plot data mainly included typical conifer-dominated (pine n = 269, spruce n = 165, other species n = 38) managed forests with relatively high LiDAR-based cover estimates (40%–99%). The LiDAR data were obtained using the ALTM 1233 scanner with a relatively low pulse density ($0.7/m^2$) and a 15° half scan angle. The FCI index, with a 1.3 m height threshold, was used as the control CC, to which the model-based CC estimates were compared. No corrections to the LiDAR-based FCI were made due to the low pulse density and the lack of scan zenith angle data.

2.7 Accuracy assessment

The statistical methodologies used for confirming the conclusions varied slightly in the sub-studies. In this summary, the accuracies of the different techniques are evaluated as in study IV, i.e. the root mean squared errors (RMSEs), biases, confidence intervals for the biases, and largest positive and negative errors are given. Assuming that the measured control values equalled the true CC at the plot, the RMSE and bias were calculated as:

$$RMSE = \sqrt{\frac{\sum_{i=1}^{n}(y_i - \hat{y}_i)^2}{n}} \qquad (3)$$

$$bias = \frac{\sum_{i=1}^{n}(y_i - \hat{y}_i)}{n} \qquad (4)$$

In equations 3 and 4, y is the canopy cover measured using the control method, ŷ is the canopy cover estimated by another method, and n is the total number of plots for which the comparison was made. More precisely, as the control result was obtained by the Cajanus tube it is not the real CC but only the best available estimate. Thus the RMSE and bias should actually be called root mean square difference and average difference, respectively. However, it is more convenient to assume that the CC control is correct and to use the well-known concepts of the RMSE and bias. The RMSD concept was only used when comparing the two control methods, dot count and LIS, to each other. Note that the commonly used notation y-ŷ in equations 3 and 4 means that if the control value is overestimated, the bias will be negative.

It was also interesting to test whether or not the biases differed significantly from zero. This was studied by calculating the 95% confidence intervals (CI) for the bias (Eq. 5):

$$CI_{bias} = bias \pm t_{\alpha/2;n-1} \frac{s}{\sqrt{n}} \tag{5}$$

where s is the standard deviation of the differences from the control, t is the critical value at confidence level α from the Student's t distribution, and n is the number of plots where the comparison was made. The lower and upper confidence limits are denoted as L_{min} and L_{max}. The largest over- and underestimations were also important criteria for the evaluation. At the individual plot level, an error smaller than 10% was considered to be a good result, while errors larger than 15% indicated low reliability. All error percentages presented in this summary and the sub-studies are absolute errors (i.e. percentage points); relative errors (i.e. the absolute error divided by the mean of the reference attribute) were not used.

The theoretical precision of the dot count estimates was assessed using binomial distribution. Because of the systematic sampling scheme and the spatial autocorrelation, the variance estimates were not unbiased, but the theoretical values still offer an interesting approximation. If the observations were uncorrelated, the variance of the estimated CC at an individual plot could be estimated as:

$$\hat{\mathrm{var}}(\hat{C}C) = \frac{\hat{C}C(1-\hat{C}C)}{n} \tag{6}$$

where n is the number of Cajanus tube measurements. In the case of a finite population size, such as in the reduction of the point density from n=195, the sample variance was calculated as (Thompson 2002, p. 40):

$$\hat{\mathrm{var}}(\hat{C}C) = \left(\frac{N-n}{N}\right)\frac{\hat{C}C(1-\hat{C}C)}{n-1} \tag{7}$$

where n is the sample size and N the population size. The theoretical RMSE (i.e. the standard error of the mean) was calculated from the mean of the individual plot variances:

$$RMSE_{theor} = \sqrt{\overline{\hat{\mathrm{var}}(\hat{C}C)}} \tag{8}$$

where $\overline{\hat{\mathrm{var}}(\hat{C}C)}$ is the mean of the plot-wise variance estimates.

3 RESULTS

3.1 Ground measurement techniques

3.1.1 Comparison of the two control methods

The combined results from studies I, III and IV are shown in Table 4. First, it is interesting to compare the results from 195 points dot count grid to the LIS estimates from the same transects. The RMSD between the 195 points dot count and the LIS method was 2.5%, the mean difference was near zero (0.3%), and the largest difference was 5.4% (Table 4). The theoretical standard deviation of the 195 point estimate is at maximum 3.6% (Eq. 6, CC = 50%). When the CCs at the individual plots are included, the theoretical RMSE (Eq. 8) is slightly smaller, 3.3%. The observed RMSD between the dot count and LIS methods is close to this value, but, as the same transects were used, the estimates are not independent and cannot be directly compared. Still, both methods should produce a reasonably accurate control value. Actually, the LIS method could be more accurate on some occasions as all gaps at the transects were recorded at a 10 cm resolution. On the other hand, the LIS method requires that all of the start and end points of continuous canopy areas are recorded without bias. Thus, the dot count method could be considered as slightly less subjective and easier to explain to new workers, as the number of unclear sample points is usually small.

3.1.2 Cajanus tube and spherical densiometer with lower sampling densities

The RMSEs obtained by systematically reducing the 195 point dot count data to 102, 49, and 23 points were 1.5%, 4.7% and 7.4%, respectively (Table 4). The largest bias was 1.6%, and the zero bias always remained well within the confidence interval. If these point densities were sampled from an infinite population (as was done for the 195 points data), the theoretical worst case standard deviations (Eq. 6, CC = 50%) would be 5.0%, 7.1% and 10.4%, respectively. However, as the samples originated from a finite population with N = 195, equations 7 and 8 must be used instead. The theoretical RMSEs obtained this way were 3.2%, 5.7%, and 9.2%, respectively, i.e. clearly larger than the empirical RMSEs. For comparison, the same analysis was repeated by using simple random sampling (SRS) without replacement instead of systematic sampling. The SRS was repeated a hundred times for each plot, and the mean variance was used in the calculations. The empirical RMSEs obtained this way were close to the theoretical RMSEs (3.0%, 5.5%, and 8.6%, respectively). Thus, in this case, the systematic data reduction produced better estimates than the reduction by SRS. The effect of systematic sampling from a finite population, together with the initial uncertainty of the 195 points estimate, explains why the observed RMSEs differ from the standard binomial theory.

The spherical densiometer produced systematically worse results than the Cajanus tube when the entire data set was considered (study I). However, when the seedling stands were omitted (Table 4), the situation was reversed: the RMSEs for 49, 23, and 9 point grids were 4.6%, 5.2%, and 6.9%, respectively. The removal of the seedling stands where the CC was usually heavily underestimated revealed that the bias of the most reliable grid, the 49 points grid, was rather small (-2.2%), but the L_{max} of the bias was only barely above zero (0.1%). For the Cajanus tube with 49 points, the bias was only -0.2%, i.e. the use of the densiometer with 20° AOV increased the overestimation by 2% points.

Table 4. Combined results from studies I, III, and IV. The control method in study I was the Cajanus tube dot count with 195 points per plot, and in studies III and IV LIS with 3 m line intervals was used. Negative numbers indicate overestimation.

Study	Method	Sample size	n	RMSE	Bias	Bias L_{min}	Bias L_{max}	Min	Max
I	Cajanus tube, LIS		19	2.5	0.3	-1.0	1.5	-4.0	5.3
	Cajanus tube, dot count	102	19	1.5	-0.4	-1.1	0.4	-3.0	3.4
	Cajanus tube, dot count	49	19	4.7	-0.2	-2.5	2.1	-8.4	8.5
	Cajanus tube, dot count	23	19	7.4	1.6	-2.0	5.2	-14.4	16.0
	Densiometer, 20°	49	15	4.6	-2.2	-4.6	0.1	-8.0	6.7
	Densiometer, 20°	23	15	5.2	-1.5	-4.3	1.4	-8.1	8.4
	Densiometer, 20°	9	15	6.9	-0.6	-4.6	3.3	-12.7	13.3
	Densiometer, subjective, 20°	10	15	7.1	3.4	-0.1	7.0	-5.5	18.6
	Ocular A		14	7.7	-0.8	-5.4	3.8	-13.7	13.2
	Ocular B		19	10.7	6.4	2.1	10.6	-8.5	24.8
	Ocular C		19	19.1	16.2	11.2	21.2	-6.5	36.2
	Canopy image, 63×49°	5	14	14.3	9.4	3.0	15.8	-9.9	32.2
	Painted canopy image, 63×49°	5	14	8.4	-4.5	-8.7	-0.2	-16.1	8.9
III	Crown relascope	1	73	9.3	-3.1	-5.1	-1.0	-24.5	18.6
IV	Automated image analysis, 1°	9	95	16.8	4.4	1.1	7.7	-34.4	48.2
	Automated image analysis, 5°	9	95	15.2	4.9	2	7.9	-31	43.7
	Automated image analysis, 10°	9	95	13.5	4.5	1.9	7.1	-28.1	33.3
	Automated image analysis, 15°	9	95	12.2	4	1.6	6.3	-25.5	30.1
	Automated image analysis, 20°	9	95	10.8	3.3	1.2	5.4	-23.1	28.2
	Automated image analysis, 25°	9	95	9.6	2.4	0.5	4.3	-20.7	26.1
	Automated image analysis, 30°	9	95	8.7	1.5	-0.3	3.2	-19.4	23.9
	Automated image analysis, 35°	9	95	7.9	0.5	-1.2	2.1	-19.7	21.7
	Automated image analysis, 40°	9	95	7.4	-0.6	-2.1	0.9	-21.2	19.0
	Automated image analysis, 45°	9	95	7.2	-1.5	-3	-0.1	-22.1	16.8
	Automated image analysis, 50°	9	95	7.2	-2.3	-3.7	-0.9	-22.8	15

The results of the subjective sampling with the densiometer in the mature stands (Table 4) were slightly worse than with the nine point systematic grid (RMSE 6.9% vs. 7.1%, bias 3.4% vs. -0.6%, respectively). Apparently, the subjective points were more frequently located in open places, especially in dense stands where taking readings under the canopy could be difficult because of low-reaching branches and thickets. This is the most likely explanation for the underestimation of the CC. However, when seedling stands were included (study I), the results of the subjective sampling appeared to be better because the mensuration problems at the seedling stands could be compensated by visual judgment.

3.1.3 Digital cameras

The first thing that was learned from the use of the point-and-shoot cameras in study I was that the within-crown gaps had a considerable effect on the CC estimates from the images (i.e. they measured canopy closure, not canopy cover). When the seedling stands were ignored, the plain thresholded canopy images underestimated CC by 9.4%, but when the within-crown gaps were painted over, the underestimation became a 4.5% overestimation (Table 4). The CIs show that both biases were statistically significant. Despite the overestimation, the painted images produced a moderate RMSE of 8.4% and the largest error was no more than 16.1%. Thus, there was room for further tests, which are presented in study IV.

The first aim of study IV was the development of an automated procedure for analyzing the skyward-looking canopy images. The Matlab script described in section 2.3.3 proved to be capable of replacing the time-consuming manual processing. The image-by-image comparison using images from the Koli site revealed that the RMSE of the automated script compared to manual processing was 2.3% and the bias was only -0.2% when a disc-shaped structuring element with a 10 pixel radius was used with the 640 × 480 pixel images. This difference was so small and the saving of time so large that it is clearly not worthwhile processing images manually (except for comparison) if the possibility of automated analysis exists. An additional benefit was that the script could be modified so that instead of analyzing the whole rectangular image, a circular part of it defined by a given AOV could be used. Thus, it was possible to easily study the effect of different AOVs just by modifying the script. These results are also given in Table 4.

The plot size and sampling scheme in study IV varied between the Koli and the test data. However, nine images per plot were taken in both data sets, and, as the number of possible sample points (images) can be considered infinite regardless of the plot size, the data from all sites are combined in Table 4. The data included a few young stands (smallest mean height 6.5 m) but in a larger data set their influence was negligible, so there was no need to exclude outliers. The best results were obtained with the largest AOVs. For example, with a 40° AOV the automated image processing was practically unbiased (-0.6%) with an RMSE of 7.4% when compared to the Cajanus tube. This result is slightly worse than that with the 20° densiometer in study I, but it must be remembered that the data used in study IV was much more versatile than the 19-plot Suonenjoki data, from which the four seedling stands were removed. The separate comparisons in study IV revealed that at the Koli site the RMSE of the automated camera method at 40° was only 4.7%, but in the test data it was 8.3%. The biggest errors occurred at sites where the stand structure was heterogeneous, typically if the vegetation at the plot center differed from the surroundings. This could have been avoided by moving some of the image points further away from the plot center.

In addition, there was an interesting trend in the development of bias when the AOV was increased from 1° to 50° (Table 4). When just the sample point was considered (AOV=1°), CC was underestimated by 4.4%, but with the increasing AOV, the bias reached zero between 35° and 40°. When the AOV was increased even more, the expected overestimation of CC started to emerge. The increase in estimated CC is natural, but the one degree measurement should actually be unbiased, even with just nine points. The likely reason for this was the rule that images should not be taken closer than 50 cm from the nearest stem, because large stems near the camera hide a large proportion of the surrounding canopy. In addition, the image locations were slightly subjective. Directions to the sampling point were determined using a compass, and the distance by 1 m steps. These reasons probably contributed to the bias in the image locations towards canopy gaps.

Study IV also considered the required sample size. The required number of images needed for reliable results depended on the stand structure. More images were needed in sites with large between-image variances in CC; these were typically places where CC was near 50%, the trees were not very tall, and the height of the living base of the crown was low. Thus, many images had a CC close to 100%, whereas the others showed only sky. Study IV indicated that in sites like these, more than 40 images per plot may be needed for reliable estimates. On the other hand, in homogeneous stands where the CC is near zero or 100%, a single image may be enough. Generally, these results indicated that an adequate sampling density would be 20–40 images per plot if the AOV was 30–40°. This could be too much for easy sites, but in any case it should not produce very large errors. Attention should also be paid to the unbiased selection of the image locations.

3.1.4 Crown relascope

The tests with the crown relascope (CBAF=250) in study III revealed that the relascope estimates had a high correlation with the Cajanus tube measurements ($R^2=0.83$). The RMSE was 9.3%, which is comparable to the other quick mensuration techniques presented here (Table 4). The negative bias of -3.1% with the CI [-5.1, -1.0] differed significantly from zero. This overestimation was expected as the assumptions of crown circularity and the lack of crown overlap were not met in practice. The results would probably have been better if the data had been restricted to stands without crown overlap, but the degree of overlap was not evaluated in the field and therefore such a test could not be performed. It was also impossible to deduce the reasons for errors at the individual plot level, but typically the errors were large for young stands, which more frequently had a clumped spatial structure and significant crown overlap. One problem in this comparison was the fixed CBAF: for example, from a 12.5 m distance, the crown width had to be 3.9 m or more to be included in the CBAF=250. Thus, if the crowns were small, the results only represented the central part of the plot, which contributed to the large errors for the young stands.

3.1.5 Ocular estimation

Finally, the results of the ocular estimation in study I and the NFI training days are given in Table 4 and Figure 9. In study I, the author's (ocular A) RMSE was 7.7% and the estimates were practically unbiased. The NFI group leaders, however, underestimated CC heavily (RMSEs 10.7% and 19.1%, biases 6.4% and 16.2% for B and C, respectively). The results clearly indicated that the experience gained from earlier plots helped to provide unbiased

estimates. It was clear that the training that B and C had received was inadequate for obtaining reliable results.

Because of these problems, every group leader visited 7–8 control plots during the NFI training days in spring 2007. This time, they were given instructions and feedback for each plot. The combined RMSE and bias histograms of this test are shown in Figure 9. The RMSEs showed a large variation (mean 8.7%, sd 2.7%), i.e. some group leaders were very good, obtaining RMSEs smaller than 5%, while the others commonly obtained errors larger than 15%. The bias histogram again shows that underestimation was more common than overestimation (mean 3.8%, sd 2.9%). It seems that it is difficult to observe the true width of the crowns from the ground, and the CC is therefore easily underestimated. Thus, it is clear that training and previous experience are needed if ocular estimations are to be used in practical inventories.

3.2 Statistical models

The development of statistical CC models in study II started with an analysis of the correlations between CC and the possible predictor variables. Strong but nonlinear relationships were found, and, as expected, the basal area showed the highest correlation with CC. When the same analysis was repeated with the whole data set of 236 plots (Fig. 10a), the basal area still had a strong correlation with CC, but the correlation with tree height was less clear (Fig. 10b). This is natural, as height alone does not indicate how many trees there are at a plot. Height information could nevertheless be utilized as a predictor.
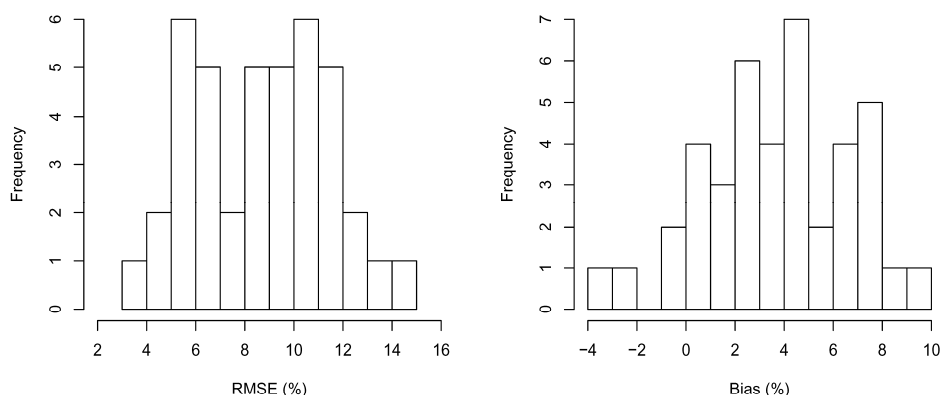

Figure 9. RMSE and bias histograms from ocular estimations during the Finnish NFI training days.
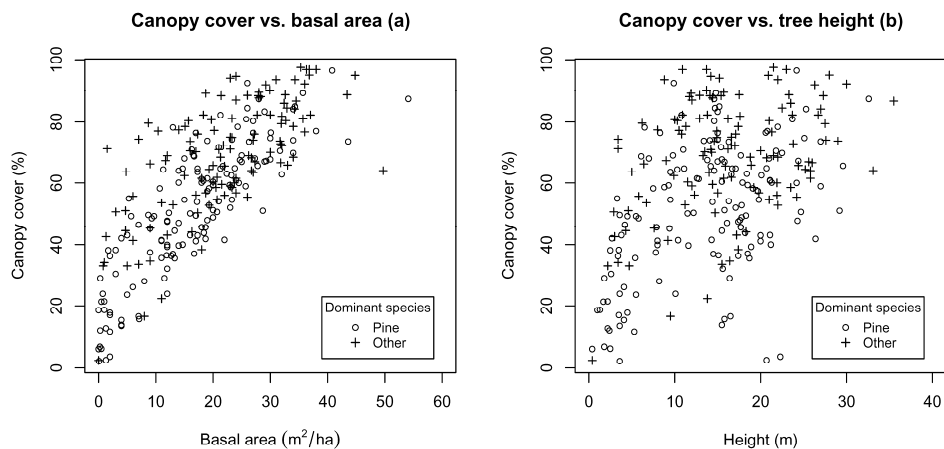
Figure 10. A scatterplot of canopy cover against basal area (a) and mean height (b).

Several models were fitted and tested in study II. The model that was best suited for practical use was the standard model, which had basal area and tree height as the general predictors (Table 5). In addition, dummy variables for unusually fertile and poor site types were included in the pine model (converted to equivalent taxation classes in Table 5) and the percentage of hardwoods were included in the spruce model. Because of the strong nonlinear relationships, the cubic form of basal area was used as the predictor as the model fit obtained this way was considerably better than with the linear or quadratic forms. For the Norway spruce model, height was also included as a cubic polynomial, but for the Scots pine model the cubic form of height did not significantly improve the model. The standard errors of the pine and spruce models were 6.3% and 5.9%, respectively, indicating a relatively good model fit. In the cross-validation test the errors increased to 7.0% and 6.8%, which are better indicators of the model's precision in real applications.

The interpretation of the Suonenjoki model coefficients revealed that increasing the basal area led to an increase in the predicted CC, as expected. Conversely, the effect of increasing the height on the predicted CC was negative in both models, i.e. for a constant basal area, taller stands had a lower CC than young stands with smaller trees. This is in fact logical, as a young stand with a basal area of 20 m^2/ha would be very dense, but in a mature stand a relatively low tree density would accumulate the same basal area. This result is typical for Finnish managed forests, where thinnings decrease CC during the rotation. In undisturbed stands, the height coefficient could also be positive if the increase in CC due to the radial growth of the crowns exceeded the increase in the gaps due to natural mortality. The fertile site dummy coefficient was positive and the poor site dummy coefficient negative, i.e. the poor site logically meant a lower CC and the fertile site a larger CC. The coefficient of the hardwood percentage was also positive, which is explained by the fact that deciduous species generally have wider crowns than pines or spruces of a similar size.

The nationwide CC models were made separately for Scots pine and the other species using the combined data from all study sites. The results are shown in Table 5 and Figure 11. The model shape was similar to the standard model, i.e. the cubic form of the basal area and tree height (quadratic form in the model for the other species) were the most significant predictors. Additional predictors included the percentage of hardwoods, north coordinate,

and taxation class. The relationship of the CC with the basal area and hardwood percentage was still positive, and with the height it was negative. The north coordinate coefficient was also negative as forests in Northern Finland are typically less dense and the crowns are narrower. The taxation class coefficients were also logical: positive for classes more fertile than the most common class (pine: II, i.e. *Vaccinium* type; other species IB, i.e. *Myrtillus* type) and negative for the less fertile classes. The model standard and cross-validation errors were 1.3%–2.6% larger than the errors of the local Suonenjoki models as the base data of the nationwide model were considerably more diverse with different species compositions, site types and geographical areas. The fitted vs. the observed value scatterplots (Fig. 11) show that some outliers remained in both models. In particular, the low end of the other species plot has some large residuals, but in practice this should not be a very large problem as the fertile sites where Norway spruce or deciduous species usually dominate quickly develop a fairly high CC.

Table 5. Canopy cover models based on the Suonenjoki and nationwide data sets.

	Suonenjoki		Nationwide	
	Pine	Spruce	Pine	Other
Constant	-1.1194	–0.48019	3.7649	4.7275
G	0.23663	0.32488	0.22080	0.18576
G^2	-0.0038168	-0.0093056	-0.00509344	-0.0031324
G^3	9.2475×10^{-6}	0.00011171	0.0000505010	0.000022933
H	-0.095561	-0.15779	-0.0701077	-0.1134
H^2		-0.002459		0.0011494
H^3		0.00015333		
HW		1.5203	1.5863	1.3662
WGSN			-0.078522	-0.083663
IA				0.29471
IB	0.16055		0.26180	
II				-0.3755
III	-0.30635		-0.17353	-0.57567
IV			-0.55582	
WL			-1.2818	
φ	55.619	55.986	33.842	28.413
R_p^2	0.914	0.871	0.871	0.798
s.e. (%)	6.3	5.9	7.7	7.8
CV s.e. (%)	7.0	6.8	8.3	9.4
AIC	-131.9	-127.0	-321.0	-257.3

Abbreviations: G, basal area (m^2/ha); H, mean height (m); HW, hardwood percentage (in hundredths); WGSN, north coordinate (WGS84); IA-IV, taxation classes from most fertile to least fertile; WL, wasteland (yearly growth less than 0.1 m^3/ha); φ, model precision parameter; R_p^2, pseudo coefficient of determination; s.e., residual standard error; CV s.e., cross-validated standard error; AIC, Akaike information criterion.
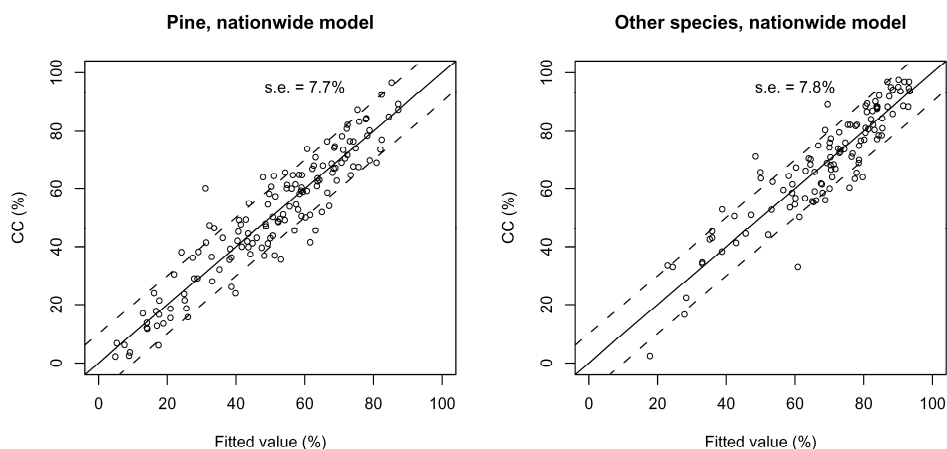
Figure 11. Fitted values versus observed canopy cover for the nationwide models. The dashed lines show 10% error limits.

3.3 Airborne laser scanning

The main results from the airborne LiDAR tests in study V are given in Table 6. The simple proportion of first and single-canopy echoes (FCI) estimated the CC with very a high precision (RMSE 3.7%), especially at the Koli site. The 3.1% overestimation due to the oblique scan zenith angles explains most of the RMSE. The FCI results for the Hyytiälä 2007 scan were not as good (RMSE 7.0%, bias -4.6%), mainly because of the ALS50-II scanner that produced dense, unevenly distributed point clouds near the maximal scan angle (study V, Fig. 6). In addition, the field control values appeared to be less accurate in the plots where crown radius measurements were used instead of the LIS method as the three largest errors occurred in these plots. Inaccuracies in tree position data could have contributed to the errors, but it is more likely that the four perpendicular crown radius measurements did not describe the horizontal crown shape well enough.

The Hyytiälä 2008 1 km scan was clearly not suitable for CC estimation (RMSE 12.5%, bias -9.2%). The explanation for this is clearly the large 32° half scan angle, which led to large strip intervals where most plots were only seen in a large side-view.

The decimation of the LiDAR data to a density of one pulse per square meter (which is close to the typical density in practical forest inventories) decreased the bias at Koli by 1%, but in the Hyytiälä 2007 and 2008 data this was decreased by 4.5% and 2.9%, respectively. Selecting just one random echo from each cell clearly decreased the point density in the crown cells, thus creating a more evenly distributed point cloud. The decimation particularly helped at Hyytiälä, where the horizontal point distributions were sometimes uneven.

Table 6. Comparison of the different LiDAR-based CC estimates to the Cajanus tube results. All numbers are percentage points.

		FCI	FCI 1m	CHM raw 0.5 m	Morph. method	FCI nearest strip	FCI nearest strip corrected
Koli	RMSE	3.7	3.4	6.6	4.6	3.5	
n=30	Bias	-3.1	-2.1	-6.0	0.9	-2.9	
	Bias L_{min}	-3.9	-3.1	-7.1	-0.8	-3.6	
	Bias L_{max}	-2.3	-1.1	-5.0	2.6	-2.1	
	Min	-7.7	-7.5	-11.7	-12.2	-7.2	
	Max	0.6	2.7	-0.9	10.8	0.5	
Hyytiälä07	RMSE	7.0	4.3	8.8	4.9	4.1	3.5
n=22	Bias	-4.6	0.1	-7.6	-1.5	-2.2	0.9
	Bias L_{min}	-6.9	-1.8	-9.6	-3.6	-3.8	-0.6
	Bias L_{max}	-2.2	2.1	-5.6	0.6	-0.6	2.5
	Min	-20.7	-12.9	-22.4	-8	-14.2	-9.0
	Max	1.6	6.9	-0.4	5.8	2.7	6.5
Hyytiälä08 1km	RMSE	12.5	9.9	15.3[a]	9.4[a]	12.9	5.0
n=18	Bias	-9.2	-6.3	-13.1[a]	3.8[a]	-9.4	-0.1
[a]n=10	Bias L_{min}	-13.5	-10.2	-19.1[a]	-2.7[a]	-13.9	-2.6
	Bias L_{max}	-4.9	-2.4	-7.0[a]	10.3[a]	-4.9	2.5
	Min	-28.1	-23.0	-26.6[a]	-8.0[a]	-29.0	-11.7
	Max	1.6	6.1	-2.6[a]	23.8[a]	1.6	8.1

Abbreviations: FCI, proportion of first and single-canopy echoes above 1.3 m; FCI 1 m, FCI calculated by selecting a random echo from each 1 m grid cell; CHM raw, FCI calculated by selecting the highest echo from each 0.5 m grid cell.

When the highest echo was selected to create the CHMs at the typical resolution of 0.5 m (Table 6, column CHM raw), the overestimation actually increased by several percent when compared to the simple FCI. If the initial CHM was processed further by filling empty cells and other outlier values, the overestimation of the CC increased even more. The CHM overestimation can probably be explained by the horizontal expansion of the crowns due to the relatively coarse resolution – a single-canopy echo at the edge of the 0.5 m cell classified the entire 0.25 m^2 area as canopy.

The morphological method can be used to create canopy maps with a considerably higher resolution (0.1 m) as the opening and closing operations will automatically process the empty cells that are left between the filled canopy cells. The advantage of the higher resolution is considerable as the morphological method had the smallest bias out of all of the methods that can be used without pulse angle data (0.9% – -3.8%). At the Koli site, the morphological method actually had a larger RMSE than the simple FCI index (3.7% vs. 4.6%), and also larger minimum and maximum errors. At some of the Koli plots, the size of the structuring element was slightly too large, which led to a loss of detail in the canopy maps and thus to a larger RMSE.

The use of just the nearest LiDAR strip echoes instead of all of the echoes did not function quite as well as expected. The decrease in bias when compared to the standard FCI was largest with the Hyytiälä 2007 data, -2.4%. At the Koli site the bias hardly decreased at all, and, most interestingly, with the Hyytiälä 2008 data it actually increased slightly. This anomaly was mainly caused by an outlier plot that was adjacent to an open area. The pulses arrived at a 31° angle from the open side, penetrating under the spruce crowns which started at a 15 m height. At the opposite forested side of the plot, the pulses arrived at a 22° angle, but they had a considerably smaller likelihood of reaching the forest floor due to a larger amount of shadowing. This problem was emphasized by the scanner that produced a much higher point density near the edge of the field-of-view than at the nadir.

The best results at the Hyytiälä site were obtained by correcting the estimates based on the nearest strip with a regression model (bias = -0.0253 × scan zenith angle × maximum height) that was fitted into the strip-wise errors with a 4.5% standard error. When the FCI was corrected by adding the predicted error, even the 2008 1 km LiDAR data produced unbiased results, and, furthermore, the 2007 RMSE decreased to 3.5%. Unfortunately, this model could not be tested using the Koli data that did not include pulse angles.

3.4 Validation of nationwide canopy cover model with airborne LiDAR data

The small RMSE between the Cajanus tube measurements and the airborne LiDAR data indicates that LiDAR data can be used as a source of validation data instead of the Cajanus tube. Thus, it was interesting to compare the predictions of the nationwide CC model to the LiDAR-derived FCI in the Matalansalo test area. The results of this test are shown in Figure 12. The pine model underestimated LiDAR-based FCI by 3.7% with an RMSE of 8.2%, while for the spruce model RMSE and bias were 9.1% and 4.2%, respectively. The RMSE values are similar to the estimates obtained in the cross-validation (8.3% and 9.4%). The results of study V showed that for the ALTM 3100 (a newer version of the ALTM 2033, used in Matalansalo), with a similar point density, the FCI typically overestimated CC by 1% – 3%, so the bias should actually be slightly smaller. Unfortunately, the Matalansalo data also lacked pulse angles, so the correction models could not be applied.

All in all, the results indicate that the models are adequate for CC estimation, at least in eastern parts of Finland, where most of the modeling data originated from. Nevertheless, at 34 out of 472 plots the model errors were larger than 15%, which should be avoided. Most of the plots with large errors appeared as outliers in the FCI – basal area scatterplot. The site types and tree heights at these plots were not particularly different, indicating that the reason for the errors could have been an unusual spatial arrangement of the trees.
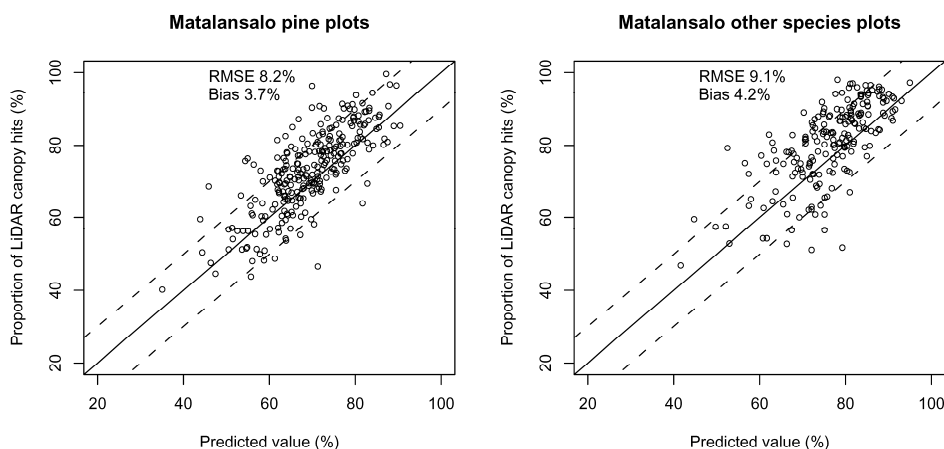
Figure 12. Comparison of nationwide CC model predictions to the LiDAR-based proportion of canopy echoes (FCI). The dashed lines show 10% error limits.

4 DISCUSSION

All of the different methods presented in this study can be used for CC assessment. Nevertheless, it is clear that the different methods have different precisions and biases, and some of them are not suitable for all situations. Canopy cover estimation *in situ* is essentially a sampling problem – if the area of interest is evenly covered with vertical observations of the canopy presence, the results should be good. It is also very important that the sampling strategy used to select the observation points is unbiased.

Vertical dot count or LIS measurements with the Cajanus tube or other instruments provide theoretically unbiased estimates of CC (as long as the sampling is unbiased) and were thus chosen for the control method. Although the determination of crown edges was sometimes subjective, the results of this work support those of earlier studies which found that dot count and LIS measurements are reliable alternatives if precise and unbiased CC estimates are needed (Johansson 1958, Jennings et al. 1999, Rautiainen et al. 2005). In particular, when compared to the CC estimated by the LIS and dot count measurements in study V, the errors of the LiDAR-based FCI index were notably small, indicating that the control values were also reasonably precise. Conversely, the attempt to measure CC based on four crown radius measurements per tree led to some exceptionally large outliers when the results were compared to the LiDAR data. Since the literature also indicates that the crown radius method may sometimes produce inaccurate results (Lang and Kurvits 2007, Ko et al. 2009), the use of dot count or LIS methods when precise CC estimates are needed should be preferred, unless time is a problem. These methods work in all forests, regardless of the crown structure, as long as vertical observations are used, the sampling is unbiased, and the measurement taker is given detailed instructions on how to work in unclear situations. Crown radius measurements for all trees in the plot are even more laborious than the dot count and LIS measurements, so they should only be used when the crown widths or *in situ* canopy maps are needed.

The good agreement between the dot count and LIS measurements also indicates that if LiDAR data are available, very detailed ground measurements are needed for obtaining results that are as good as the simple proportion of (first and single) canopy echoes, which can be easily derived from LiDAR data. This simple index can be used if the typical bias of 1–5% is acceptable or if it can be corrected. The scale of the bias mainly depends on the scan zenith angle but also on the echo density and horizontal sampling pattern, and the sensor properties could also influence the results. Different methods for correcting the bias were tested in study V, and of these the use of scan zenith angle and normalized pulse heights to create models for correcting the bias provided the best results. However, the use of the correction models should be further tested in the future. Of the other bias correction methods, the point cloud decimation and morphological canopy mapping methods provided the best results, but in real applications it could be simpler to just estimate the scale of the bias and subtract it from the FCI. Carefully measured field data are certainly useful for validating LiDAR-based CC estimates, but these results indicate that regression calibration may not always be necessary.

The results show that the LiDAR-based techniques were the only ones that were capable of producing CC estimates that normally differed by less than 10% from the Cajanus tube estimate. However, in practical inventories, LiDAR data are not always available. The quicker field methods and statistical modeling remain as alternatives for the laborious sighting tube sampling. If there are 2–10 minutes available for the CC measurement, measuring approximately 10–30 sample points with a narrow AOV (30°–40°) instrument, such as a digital camera or a spherical densiometer, should produce fairly reliable CC estimates. These results indicate that with small AOVs the number of sample points can be reduced significantly, and the overestimation should remain relatively small. A more difficult problem could be guaranteeing that the sampling scheme was unbiased. Systematic samples as such may be biased in forests with regular tree patterns, but the sampling should still cover the entire plot, so few other options remain. For the best possible precision, a tape measure or some other distance measuring device should be used to ensure that the sample points are where they should be, but in practice it may be that time limits exclude this option.

Digital cameras, densiometers, and moosehorns with narrow AOVs should all be valid instruments for CC measurements. The main advantage of using a digital camera is that taking images is faster than calculating the grid coverage with the densiometer. The densiometer is simple, portable and gives the result immediately, but it is slower to use and the mensuration may be prone to errors. With the camera, images are saved as documents for later inspection and their automated analysis was reliable. In addition, the AOV to be used in the analysis can be set by the operator, so it is also possible to simulate dot count measurements with the camera. The Matlab scripts used in study IV are also freely available for download (Heikkinen and Korhonen 2009). Nowadays, basic point-and-shoot digital cameras cost even less than a spherical densiometer (less than €100), and thus price should not be an obstacle. One restriction is that the sun should not appear in the images because nearby pixels will become saturated. This could be a problem near the equator where the sun rises high enough to appear in the images. However, sunlit crowns in the images can usually be processed without problems. The problem with all AOV measurements are seedlings stands – if the CC is required exactly as the definition states, the images should actually be taken at ground level. In such places, the use of AOV measurements instead of the sighting tube is questionable.

The crown relascope measurements typically take 1 – 4 minutes, depending on the number of trees to be evaluated. Thus, the crown relascope could be used as an alternative to quick AOV measurements in forests where the canopy structure is favorable, i.e. the visibility is good, the crowns do not overlap frequently, and the horizontal crown shape is near circular. It is important to select the CBAF based on the average crown width so that a single measurement covers the entire plot. The crown relascope could be particularly useful in the FAO forest classification, as it is easy to use the CBAF = 100 and to calculate whether or not there are more than ten trees (10% CC) at the sample plot, provided that the conditions mentioned above are fulfilled.

If the time available for CC measurements is less than a minute per plot, the remaining alternatives include ocular estimation and the use of regression models based on the available stand characteristics. This is the situation in the Finnish NFI, where the practical alternatives for CC estimation are modeling, the ocular method, and sometimes the crown relascope. The results of the ocular estimation test in study I showed that proper training of the observers is needed. Nevertheless, the results from the NFI training days showed that after detailed instructions and training, some group leaders reached a precision nearly equal to the LiDAR or Cajanus tube results. However, the range of RMSEs was 4% – 15%, and CC was commonly underestimated by up to 10%. Loetsch et al. (1973) wrote that ocular observers commonly underestimate CC, and it seems that their statement is still valid. Ocular estimation can be used as a last option if other methods cannot be used, but decent training and monitoring of results is essential.

The RMSE of the nationwide CC models at the Matalansalo test site and in the cross-validation test was approximately 8% – 9.5%, so the model is more reliable than an untrained ocular observer, but with decent training this situation could change. The model can still be used if there is no time for separate measurements, or for auxiliary information before an ocular estimation, or even afterwards as an alternative estimate. A possible way of improving the performance of this model could be the inclusion of a spatial index as a predictor variable, if these data were more commonly available.

In the future, modeling data should be extended further, which would be easiest to accomplish by using angle-corrected LiDAR data to avoid the time-consuming Cajanus tube measurements. The current data set is focused on eastern Finland, so more data should be obtained from other parts of the country. The plots were subjectively located in order to maximize the diversity of the data and they also included at least a few plots from relatively rare forests, such as the low CC spruce stands. Still, it would be better to obtain additional plots with a more objective sampling scheme. A larger database would also enable the use of nonparametric estimation, such as nearest neighbor methods. The use of the crown radius approach (Gill et al. 2000) with the help of spatial structure models (e.g. Tomppo 1986) is one alternative that should be studied in future, and also in boreal forests, although the results in other parts of the world have not been very good so far (Ko et al. 2009).

The regression models presented here are not ideal for describing CC as a function of stand age because the empirical data included few cases from the first years of the rotation. The seedling stands in the modeling data usually had a well-established tree population and thus the CC had already reached 20% – 50%. In a recent study (Lohila et al. 2010), some of the same nationwide data that were used here were used to make nonlinear curves that were capable of describing the development of a typical forest during the entire rotation. On the other hand, these models could, in some cases, produce estimates outside of the standard unit interval, and thus the use of the beta regression approach is safer in situations where just an estimate of the current CC is required.

In summary, the results presented here should be valid for semi-natural boreal forests as the data included the most common forest types and development stages encountered in Finland. However, a direct comparison of the results (using RMSE or R^2 values, etc.) to other recently published studies (Fiala et al. 2006, Ko et al. 2009, Paletto and Tosi 2009) was not feasible as the results came from structurally different forests and the range of CC values may differ considerably in different types of forests. Even though the precisions of individual methods cannot be generalized, the sighting tube methodology as presented here should be applicable everywhere, and, furthermore, the AOV and crown relascope methods can be applied reliably if the prerequisites described above are met. However, all studies agreed that the different mensuration devices yielded different results, mainly because of different AOVs and inclusion or exclusion of within-crown gaps. It is up to the inventory designers to select the most appropriate method based on their needs. In many cases canopy closure could be a more descriptive variable than CC, for example if the light conditions under the canopy were the parameter of interest.

The interest in forest canopy structure will probably continue to increase in the future. Canopy cover data are required for monitoring large scale forest areas, but also at local scales down to the individual plot level for different ecological applications. The field methods presented here are valid for traditional forest inventories and more ecologically oriented campaigns where CC is required, usually as one of several variables of interest. If CC is considered important, then enough time and resources should be allocated to guarantee an adequate sampling density.

The plot inventories only produce a sample of the CC in the area of interest. If wall-to-wall coverage is necessary, the use of different remote sensing methods is the only alternative. The availability of different remotely sensed data has increased drastically over the past ten years, and the price has decreased substantially. This development is likely to continue in the future. For instance, UAVs (unmanned aerial vehicles) suitable for small-scale aerial photography have become commercially available and could be a good alternative to plot level CC estimations. Also, several upcoming satellite missions will provide new data sources for CC monitoring. For example, the ESA's Sentinel 2 and the German hyperspectral EnMAP (Environmental Mapping and Analysis Program) missions will increase the availability of moderate resolution optical data, while NASA's DESDyni spaceborne profiling LiDAR will provide global vegetation height measurements. Satellite sensors with a coarse to medium spatial resolution remain as the best alternative for continuous change monitoring due to their high temporal resolution, especially from the national to global scale.

However, in Finland, the airborne LiDARs could be the most practical way of providing CC data. The LiDARs are capable of producing accurate estimates from the plot to regional levels. Airborne LiDARs are already used in practical forest inventories in both private and state-owned forests, and the production of the LiDAR-based nationwide elevation model will cover the entire Finland with leaf-off LiDAR measurements over the next ten years. It is reasonable to assume that the need for *in situ* CC measurements will decrease as LiDAR data become commonly available. For instance, Graf et al. (2009) demonstrated how the LiDAR-based CC estimation was used to detect capercaillie (*Tetrao urogallus*) habitats in the Swiss Alps. However, the availability of LiDAR data will stay limited in many parts of the world, and its price is still higher than the price of aerial images or satellite data. Furthermore, field inventories are still needed to provide validation data for remote sensing, and in many parts of the world it might be easier to hire field workers than

remote sensing experts. Basic knowledge on the precision and costs of the different alternatives should in any case lead to better quality end products.

REFERENCES

Anderson, M.C. 1964. Studies of the woodland light climate: I. The photographic computation of light conditions. Journal of Ecology 52(1): 27-41.

Anderson, R.C., Loucks, O.L. & Swain, A.M. 1969. Herbaceous response to canopy cover, light intensity, and throughfall precipitation in coniferous forests. Ecology 50(2): 255-263.

Axelsson, P. 2000. DEM generation from laser scanner data using adaptive TIN models. International Archives of Photogrammetry and Remote Sensing 33: 110–117.

Bai, Y., Walsworth, N., Roddan, B., Hill, D.A., Broersma, K., & Thompson, T. 2005. Quantifying tree cover in forest-grassland ecotone of British Columbia using crown delineation and pattern detection. Forest Ecology and Management 212: 92–100.

Bechtold, W.A. 2003. Crown-diameter prediction models for 87 species of stand-grown trees in the Eastern United States. Southern Journal of Applied Forestry 27(4): 269-278.

Betts, A.K. & Ball, J.H. 1997. Albedo over boreal forest. Journal of Geophysical Research 102(D24): 28901–28909.

Bitterlich, W. 1948. Die Winkelzählprobe. Allgemeine Forst und Holzwirtschaftliche Zeitung 59(1): 4-5.

— 1961. Sclussgrad durch Winkelzählprobe. Holtz-Kurier 16(35): 7–8.

— 1984. The relascope idea. Commonwealth Agricultural Bureaux. Farnham Royal. 242 p.

Bonnor, G. M. 1967. Estimation of ground canopy density from ground measurements. Journal of Forestry 65(8): 544–547.

Buckley, D.S., Isebrands, J.G. & Sharik, T.L. 1999. Practical field methods of estimating canopy cover, PAR, and LAI in Michigan oak and pine stands. Northern Journal of Applied Forestry 16(1): 25-32.

Bunnell, F.L. & Vales, D.J. 1990. Comparison of methods for estimating forest overstory cover: differences among techniques. Canadian Journal of Forest Research 20: 101–107.

Carreiras, J.M.B., Pereira, J.M.C. & Pereira, J.S. 2006. Estimation of tree canopy cover in evergreen oak woodlands using remote sensing. Forest Ecology and Management 223: 45–53.

Cescatti, A. 2007. Indirect estimates of canopy gap fraction based on the linear conversion of hemispherical photographs. Methodology and comparison with standard thresholding techniques. Agricultural and Forest Meteorology 143: 1–12.

Chopping, M. 2011. CANAPI: canopy analysis with panchromatic imagery. Remote Sensing Letters 2(1), 21–29. First published on: 17 June 2010 (iFirst).

Christopher, T.A. & Goodburn, J.M. 2008. The effects of spatial patterns on the accuracy of forest vegetation simulator (FVS) estimates of forest canopy cover. Western Journal of Applied Forestry 23(1): 5–11.

Chubey, M.S., Franklin, S.E. & Wulder, M.A. 2006. Object-based analysis of Ikonos-2 imagery for extraction of forest inventory parameters. Photogrammetric Engineering & Remote Sensing 72(4): 383–394.

Cook, J.G., Stutzman, T.W., Bowers, C.W., Brenner, K.A., & Irwin, L.L. 1995. Spherical densiometers produce biased estimates of forest canopy cover. Wildlife Society Bulletin 23(4): 711–717.

Crookston, N. L. & Stage, A. R. 1999. Percent canopy cover and stand structure statistics from the Forest Vegetation Simulator. Gen. Tech. Rep. RMRS-GTR-24. Ogden, UT: U. S. Department of Agriculture, Forest Service, Rocky Mountain Research Station. 11 p.

Culvenor, D. S. 2003. Extracting individual tree information. A survey of techniques for high spatial resolution imagery. In: Wulder, M. A. & Franklin, S. E. (Eds.). Remote

sensing of forest environments: concepts and case studies. Kluwer Academic Publishers, Boston. 519 p.

Danson, F.M., Hetherington, D., Morsdorf, F., Koetz, B., & Allgöwer, B. 2007. Forest canopy gap fraction from terrestrial laser scanning. IEEE Geoscience and Remote Sensing Letters 4: 157–160.

FAO 2004. Global forest resources assessment update 2005. Terms and definitions (Final version). Forest resources assessment programme working paper 83/E, Rome, Italy. 36 p. Available at: ftp://ftp.fao.org/docrep/fao/007/ae156e/AE156E00.pdf. Last accessed 24.7.2010.

Fensham, R.J., Fairfax, R.J., Holman, J.E. & Whitehead, P.J. 2002. Quantitative assessment of vegetation structural attributes from aerial photography. International Journal of Remote Sensing 23(11): 2293–2317.

— & Fairfax, R.J. 2007. Effect of photoscale, interpreter bias and land type on woody crown-cover estimates from aerial photography. Australian Journal of Botany 55, 457–463.

Ferrari, S. & Cribari-Neto, F. 2004. Beta regression for modelling rates and proportions. Journal of Applied Statistics 31(7): 799-815.

Fiala, A.C.S., Garman, S.L., & Gray, A.N. 2006. Comparison of five canopy cover estimation techniques in the Western Oregon Cascades. Forest Ecology and Management 232: 188–197.

Frazer, G., Canham, C., and Lertzman, K., 1999. Gap Light Analyzer (GLA), Version 2.0: Imaging software to extract canopy structure and gap light transmission indices from true-colour fisheye photographs, users manual and program documentation. Copyright © 1999: Simon Frazer University, Burnaby, British Columbia, and the Institute of Ecosystem studies, Millbrook, New York. 36 p.

Ganey, J.L. & Block, W.M. 1994. A comparison of two techniques for measuring canopy closure. Western Journal of Applied Forestry 9(1): 21–23.

Garrison, G. A. 1949. Uses and modifications for the "moosehorn" crown closure estimator. Journal of Forestry 47: 733–735.

Gemmell, F. 1999. Estimating conifer forest cover with thematic mapper data using reflectance model inversion and two spectral vegetation indices in a site with variable background characteristics. Remote Sensing of Environment 69: 105-121.

— & Varjo, J. 1999. Utility of reflectance model inversion versus two spectral indices for estimating biophysical characteristics in a boreal forest test site. Remote Sensing of Environment 68: 95-111.

— , Varjo, J., Strandström, M. & Kuusk, A. 2002. Comparison of measured boreal forest characteristics with estimates from TM data and limited ancillary information using reflectance model inversion. Remote Sensing of Environment 81: 365-377.

Gill, S.J., Biging, G.S. & Murphy, E.C. 2000. Modeling conifer tree crown radius and estimating canopy cover. Forest Ecology and Management 126: 405–416.

GOFC-GOLD 2009. Reducing greenhouse gas emissions from deforestation and degradation in developing countries: a sourcebook of methods and procedures for monitoring, measuring and reporting, GOFC-GOLD Report version COP14-2, GOFC-GOLD Project Office, Natural Resources Canada, Alberta, Canada. 185 p.

Gonzalez, R.C. & Woods, R.E. 2002. Digital image processing. 2nd ed. Prentice Hall, Upper Saddle River, NJ. 793 p.

Graf, R.F., Mathys, L. & Bollmann, K. 2009. Habitat assessment for forest dwelling species using LiDAR remote sensing: Capercaillie in the Alps. Forest Ecology and Management 257: 160–167.

Gregoire, T. & Valentine, H. 2007. Sampling strategies for natural resources and the environment. Applied Environmental Statistics Vol. 3. Chapman & Hall/CRC. 474 p.

Gschwantner, T., Schadauer, K., Vidal, C., Lanz, A., Tomppo, E., di Cosmo, L., Robert, N., Duursma, D.E. & Lawrence, M. 2009. Common tree definitions for national forest inventories in Europe. Silva Fennica 43(2): 303–321.

Hansen, M.C., Defrıes, R.S., Townshend, J.R.G., Carroll, M., Dimiceli, C. & Sohlberg, R.A. 2003. Global percent tree cover at a spatial resolution of 500 metres: First results of the MODIS vegetation continuous fields algorithm. Earth Interactions 7(10): 1–15.

Heikkinen J. & Korhonen L. 2009. MATLAB codes for canopy image analysis. Available online at www.mathworks.com/matlabcentral/fileexchange/24314; last accessed November 10, 2010.

Heiskanen, J., Nilsson, B., Mäki, A.H., Allard, A., Moen, J., Holm, S., Sundquist, S. & Olsson, H. 2008. Aerial photo interpretation for change detection of treeline ecotones in the Swedish mountains. Sveriges lantbruksuniversitet,Arbetsrapport 242. Umeå.

Hirschmugl, M., 2008. Derivation of forest parameters from UltracamD data. Doctoral Thesis, Graz University of Technology. 238 p.

Holmgren, J., Nilsson, M. & Olsson, H. 2003. Simulating the effects of lidar scanning angle for estimation of mean tree height and canopy closure. Canadian Journal of Remote Sensing 29: 623–632.

— , Johansson, F., Olofsson, K., Olsson, H. & Glimskär, A. 2008. Estimation of crown coverage using airborne laser scanner. In: R.A. Hill, J. Rosette, & J. Suárez (Eds.). Proceedings of SilviLaser 2008: 8th International Conference on LiDAR Applications in Forest Assessment and Inventory (pp. 50–57). September 17-19, 2008, Heriot-Watt University, Edinburgh, UK.

Holopainen, M., Haapanen, R., Karjalainen, M., Vastaranta, M., Hyyppä, J. Yu, X., Tuominen, S. & Hyyppä, H. 2010. Comparing accuracy of airborne laser scanning and TerraSAR-X radar images in the estimation of plot-level forest variables. Remote Sensing 2: 432–445.

Hyyppä, J. & Hallikainen, M. 1996. Applicability of airborne profiling radar to forest inventory. Remote Sensing of Environment 57(1): 39–57.

— , Kelle, O., Lehikoinen, M. & Inkinen, M. 2001. A segmentation-based method to retrieve stem volume estimates from 3-dimensional tree height models produced by laser scanner. IEEE Transactions on Geoscience and Remote Sensing 39: 969–975.

IPCC 2003. Penman, J., Gytarsky, M., Hiraishi, T., Krug, T., Kruger, D., Pipatti, R., Buendia, L., Miwa, K., Ngara, T., Tanabe, K. & Wagner F. (Eds.). Good practice guidance for land use, land-use change and forestry. Institute for Global Environmental Strategies (IGES), Hayama, Japan.

— 2006. Eggleston, S., Buendia, L., Miwa, K. Ngara, T. & Tanabe, K. (Eds.). IPCC Guidelines for National Greenhouse Gas Inventories. Institute for Global Environmental Strategies (IGES), Hayama, Japan. 976 pages.

Jackson, M. & Petty, R. 1973. A simple optical device for measuring vertical projection of tree crowns. Forest Science 19: 60–62.

James, F.C. 1971. Ordinations of habitat relationships among breeding birds. The Wilson Bulletin 83(3): 215-236.

Jasinski, M.F. 1990. Sensitivity of the normalized difference vegetation index to subpixel canopy cover, soil albedo, and pixel scale. Remote Sensing of Environment 32(2-3): 169–187.

— 1996. Estimation of subpixel vegetation density of natural regions using satellite multispectral imagery. IEEE Transactions on Geoscience and Remote Sensing 34(3): 804–813.

Jennings, S.B., Brown, N.D. & Sheil, D. 1999. Assessing forest canopies and understorey illumination: canopy closure, canopy cover and other measures. Forestry 72(1): 59–74.

Johansson, T. 1985. Estimating canopy density by the vertical tube method. Forest Ecology and Management 11: 139-144.

Jonckheere, I., Nackaerts, K., Muys, B., Coppin, P., 2005. Assessment of automatic gap fraction estimation of forests from digital hemispherical photography. Agricultural and Forest Meteorology 132(1–2): 96–114.

Jupp, D.L.B., Culvenor, D.S., Lovell, J., Newnham, G., Strahler, A.H. & Woodcock, C.E. 2009, Estimating forest LAI profiles and structural parameters using a ground based laser called 'Echidna®'. Tree Physiology 29: 171–181.

Knowles, R. L., Horvath, G. C., Carter, M. A. & Hawke, M. F. 1999. Developing a canopy closure model to predict overstorey/understorey relationships in Pinus radiata silvopastoral systems. Agroforestry systems 43: 109-119.

Ko, D., Bristow, N., Greenwood, D. & Weisberg, P. 2009. Canopy cover estimation in semiarid woodlands: comparison of field-based and remote sensing methods. Forest Science 55(2): 132–141.

Korhonen, L., Kaartinen, H., Kukko, A., Solberg, S. & Astrup, R. 2010. Estimating vertical canopy cover with terrestrial and airborne laser scanning. Proceedings of Silvilaser 2010, Freiburg, Germany. 11 p.

Korpela, I. 2004. Individual tree measurements by means of digital aerial photogrammetry. Silva Fennica monographs 3. 93 p.

— , Tuomola, T., & Välimäki, E. 2007. Mapping forest plots: An efficient method combining photogrammetry and field triangulation. Silva Fennica 41(3): 457–469.

Kuusipalo, J. 1985. On the use of tree stand parameters in estimating light conditions below the canopy. Silva Fennica 19(2): 185–196.

Lang, M., & Kurvits, V. 2007. Restoration of tree crown shape for canopy cover estimation. Forestry Studies 46: 23-34.

Lemmon, P. E. 1956. A spherical densiometer for estimating forest overstory density. Forest Science 2: 314–320.

Liang, S. 2004. Quantitative remote sensing of land surfaces. John Wiley & Sons, Hobeken, N.J. 534 p.

Lillesand, T.M., Kiefer, R.W. & Chipman, J.W. 2004. Remote sensing and image interpretation. 5th Ed. John Wiley & Sons, New York. 763 p.

Loetsch, F. & Haller, E. 1973. Forest Inventory. Volume I. 2nd ed. BLV Verlags-gesellschaft. München. 436 s.

Loetsch, F., Zöhrer, F. & Haller, K. E. 1973. Forest inventory. Volume II. BLV Verlagsgesellschaft. 469 p.

Lohila, A., Minkkinen, K., Laine, J., Savolainen, I., Tuovinen, J.-P., Korhonen, L., Laurila, T., Tietäväinen, H. & Laaksonen, A. 2010. Forestation of boreal peatlands: Impacts of changing albedo and greenhouse gas fluxes on radiative forcing. Journal of Geophysical Research 115, G04011, doi:10.1029/2010JG001327.

Lovell, J.J., Jupp, D.L.P., Culvenor, D.S. & Coops, N.C. 2003. Using airborne and ground-based ranging lidar to measure canopy structure in Australian forests. Canadian Journal of Remote Sensing 29: 607–622.

Mäkinen, A., Korpela, I., Tokola, T. & Kangas, A. 2006. Effects of imaging conditions on crown diameter measurements from high-resolution digital photographs. Canadian Journal of Forest Research 36: 1206–1217.

Manninen, T., Stenberg, P., Rautiainen, M., Voipio, P. & Smolander, H. 2005. Leaf area index estimation of boreal forest using ENVISAT ASAR. IEEE Transactions on Geoscience and Remote Sensing 43(11): 2627–2635.

Manninen, T., Korhonen, L., Voipio, P., Lahtinen, P. & Stenberg, P. 2009. Leaf area index (LAI) estimation of boreal forest using wide optics airborne winter photos. Remote Sensing 1(4): 1380-1394.

Mathworks Inc. 2008. MATLAB – The language of technical computing. Available online at www.mathworks.com/products/matlab/. Last accessed November 26, 2010.

McCullagh, P. & Nelder, J.A. 1989. Generalized linear models, 2nd edn. Monographs on statistics and probability 37. Chapman and Hall, London. 511 p.

Mikhail, E.M., Bethel, J.S., McGlone, J.C. 2001. Introduction to modern photogrammetry. John Wiley & Sons, Inc. 479 p.

Miller, J.D., Knapp, E.E., Key, C.H., Skinner, C.N., Isbell, C.J., Creasy, R.M., & Sherlock, J.W. 2009. Calibration and validation of the relative differenced Normalized Burn Ratio (RdNBR) to three measures of fire severity in the Sierra Nevada and Klamath Mountains, California, USA. Remote Sensing of Environment 113: 645–656.

Mitchell, J. E. & Popovich, S. J. 1997. Effectiveness of basal area for estimating canopy cover of ponderosa pine. Forest Ecology and Management 95(1): 45-51.

Morsdorf, F., Kötz, B., Meier, E. Itten, K.I. & Allgöwer, B. 2006. Estimation of LAI and fractional cover from small footprint airborne laser scanning data based on gap fraction. Remote Sensing of Environment 104: 50–61.

Næsset, E., Gobakken, T., Holmgren, J., Hyyppä, H., Hyyppä, J., Maltamo, M., Nilsson, M., Olsson, H., Persson, Å., & Söderman, U. 2004. Laser scanning of forest resources: the Nordic experience. Scandinavian Journal of Forest Research 19: 482–499.

Nobis, M. & Hunziker, U. 2005. Automatic thresholding for hemispherical canopy-photographs based on edge detection. Agricultural and Forest Meteorology 128: 243–250.

Nuttle, T. 1997. Densiometer bias? Are we measuring the forest or the trees? Wildlife Society Bulletin 25(3): 610–611.

O'Brien, R.A. 1989. Comparison of overstory canopy estimates on forest survey plots. USDA Forestry Service General Technical Report INT-GTR-417. 5 p.

Ozanne, C.M.P., Anhuf, D., Boulter, S.L., Keller, M., Kitching, R. L., Körner, C., Meinzer, F.C., Mitchell, A.W., Nakashizuka, T., Silva Dias, P.L., Stork, N.E., Wright, S. J., & Yoshimura, M. 2003. Biodiversity meets the atmosphere: a global view of forest canopies. Science 301: 183–186.

Paine, D.P. & Kiser, J.D. 2003. Aerial photography and image interpretation. 2nd ed. John Wiley & Sons, Hoboken, New Jersey. 632 p.

Palace, M., Keller, M., Asner, G.P., Hagen, S. & Braswell, B. 2007. Amazon forest structure from IKONOS satellite data and the Automated characterization of forest canopy properties. Biotropica 40(2): 141–150.

Paletto, A. & Tosi, V. 2009. Forest canopy cover and canopy closure: a comparison of assessment techniques. European Journal of Forest Research 128: 265–272.

Pekin, B. & Macfarlane, C. 2009. Measurement of crown cover and leaf area index using digital cover photography and its application to remote sensing. Remote Sensing 1(4):1298–1320.

Pitkänen, J. 2001. Individual tree detection in digital aerial images by combining locally adaptive binarization and local maxima methods. Canadian Journal of Forest Research 31: 832–844.

Pouliot, D.A., King, D.J., Bell, F.W. & Pitt, D.G. 2002. Automated tree crown detection and delineation in high-resolution digital camera imagery of coniferous forest regeneration. Remote Sensing of Environment 82: 322–334.

R Development Core Team 2008. R: A language and environment for statistical computing. R Foundation for Statistical Computing, Vienna, Austria. ISBN 3-900051-07-0. URL:http://www.R-project.org, accessed 18.10.2010.

Ranius, T. & Jansson, N. 2000. The influence of regrowth, original canopy cover and tree size on saproxylic beetles associated with old oaks. Biological Conservation 95: 85–94.

Rautiainen, M., Stenberg, P., Nilson, T., Kuusk, A. & Smolander, H. 2003. Application of a forest reflectance model in estimating leaf area index of Scots pine stands using Landsat 7 ETM reflectance data. Canadian Journal of Remote Sensing 29(3): 314–323.

— , Stenberg, P. & Nilson, T. 2005. Estimating canopy cover in Scots pine stands. Silva Fennica 39(1): 137–142.

Riaño, D., Valladares, F., Condés, S. & Chuvieco, E. 2004. Estimation of leaf area index and covered ground from airborne laser scanner (Lidar) in two contrasting forests. Agricultural and Forest Meteorology 124: 269–275.

Robinson, M.W. 1947. An instrument to measure forest crown cover. The Forestry Chronicle 23: 222-225.

Sakamoto, Y., Ishiguro, M. & Kitagawa, G. 1986. Akaike information criterion statistics. KTK Scientific Publishers, Tokyo. 290 p.

Sarvas, R. 1953. Measurement of the crown closure of the stand. Communicationes Instituti Forestales Fenniae 41(6). 13 p.

Smith, A.M.S., Falkowski, M.J., Hudak, A.T., Evans, J.S., Robinson, A.P. & Steele, C.M. 2009. A cross-comparison of field, spectral, and lidar estimates of forest canopy cover. Canadian Journal of Remote Sensing 35: 447–459.

Smith, M.-L., Anderson, J. & Fladeland, M. 2008. Forest canopy structural properties. In C.M. Hoover (Ed.): Field Measurements for Forest Carbon Monitoring, pp. 179–196. New York: Springer Science and Business Media.

Song, C., Dickinson, M.B., Su, L., Zhang, S. & Yaussey, D. 2010. Estimating average tree crown size using spatial information from Ikonos and QuickBird images: across-sensor and across-site comparisons. Remote Sensing of Environment 114: 1099–1107.

Spanner, M.A., Pierce, L.I., Peterson, D.L. & Running, S.W. 1990. Remote sensing of temperate coniferous forest leaf area index The influence of canopy closure, understory vegetation and background reflectance. International Journal of Remote Sensing 11(1): 95–111.

Stenberg, P., Mõttus, M. & Rautiainen, M. 2008. Modeling the spectral signature of forests: application of remote sensing models to coniferous canopies. In S. Liang (Ed.): Advances in Land remote Sensing: System, Modeling, Inversion and Application. Springer, New York, pp. 147-171.

Stumpf, K. A. 1993. The estimation of forest vegetation cover descriptions using a vertical densiometer. Available at: http://www.grsgis.com/publications/saf_93.html. Last accessed 27 July 2010].

Suvanto, A. & Maltamo, M. 2010. Using mixed estimation for combining airborne laser scanning data in two different forest areas. Silva Fennica 44(1): 91–107.

Thompson, S.K. 2002. Sampling. 2nd ed. Wiley series in probability and statistics. John Wiley & Sons, New York. 367 p.

Tomppo, E. 1986. Models and methods for analysing spatial patterns of trees. Communicationes Instituti Forestalis Fenniae 138. 65 p.

Vales, D. J. & Bunnell, F. L. 1988. Comparison of methods for estimating forest overstory cover. I. Observer effects. Canadian Journal of Forest Research 18(5): 606-609.

Valtakunnan metsien 10. inventointi (VMI10). Maastotyön ohjeet 2008. Koko Suomi. Metsäntutkimuslaitos, Helsinki. [In Finnish]

Vaughn, N. & Ritchie, M.W. 2005. Estimation of crown cover in interior ponderosa pine stands: effects of thinning and prescribed fire. Western Journal of Applied Forestry 20(4): 240–246.

Vauhkonen, J., Tokola, T., Maltamo, M. and Packalén, P. 2008. Effects of pulse density on predicting characteristics of individual trees of Scandinavian commercial species using alpha shape metrics based on airborne laser scanning data. Canadian Journal of Remote Sensing 34: S441-S459.

Walters, J & Soos, J. 1962. The gimbal sight for the projection of the crown radius. Faculty of Forestry, University of British Columbia, Vancouver. Research note 39.

Wang, Y., Weinacker, H. & Koch, B. 2008. A lidar point cloud based procedure for vertical canopy structure analysis and 3D single tree modelling in forest. Sensors 8: 3938–3951.

Wehr, A. & Lohr, U. 1999. Airborne laser scanning – an introduction and overview. ISPRS Journal of Photogrammetry and Remote Sensing 54: 68–82.

Werner, E.E. & Glennemeier, K.S. 1999. Influence of forest canopy cover on the breeding pond distributions of several amphibian species. Copeia 1: 1-12.

Williams, M. S., Patterson, P. L. & Mowrer, H. T. 2003. Comparison of ground sampling methods for estimating canopy cover. Forest Science 49(2): 235–246.

Wilson, B. 2011. Cover plus: ways of measuring plant canopies and the terms used for them. Journal of Vegetation Science 22(2): 197–206.

Wolter, P.T., Townsend, P.A. & Sturtevant, B.R. 2009. Estimation of forest structural parameters using 5 and 10 meter SPOT-5 satellite data. Remote Sensing of Environment 113: 2019-2036.

Woodcock, C.E., Collins, J.B., Jakabhazy, V.D., Li, X., Macomber, S.A. & Wu, Y. 1997. Inversion of the Li-Strahler canopy reflectance model for mapping forest structure. IEEE Transactions on Geoscience and Remote Sensing 35(2): 405–414.

Wulder, M., Niemann, K.O. & Goodenough, D. 2000. Local maximum filtering for the extraction of tree locations and basal area from high spatial resolution imagery. Remote Sensing of Environment 73: 103–114.

Zeide, B. 2005. How to measure stand density. Trees 19: 1–14.

Zeng, Y., Schaepman, M.E., Wu, B., Clevers, J.G.P.W. & Bregt, A.K. 2009. Quantitative forest canopy structure assessment using an inverted geometric-optical model and up-scaling. International Journal of Remote Sensing 30(6): 1385–1406.